Contents

List of Figures

List of Table

Chapter-1

INTRODUCTION

Introduction

Carbon is a very important element in the periodic table that supports life on earth. Importance of carbon for many technological and industrial applications can be seen from synthetic materials to drugs. The unique property of carbon for which wide range of applications can be realize is its ability to make bonds with itself and other elements in lots of variations. The resulting molecular structures of organic compounds have a broad range of physical and chemical properties and applications.

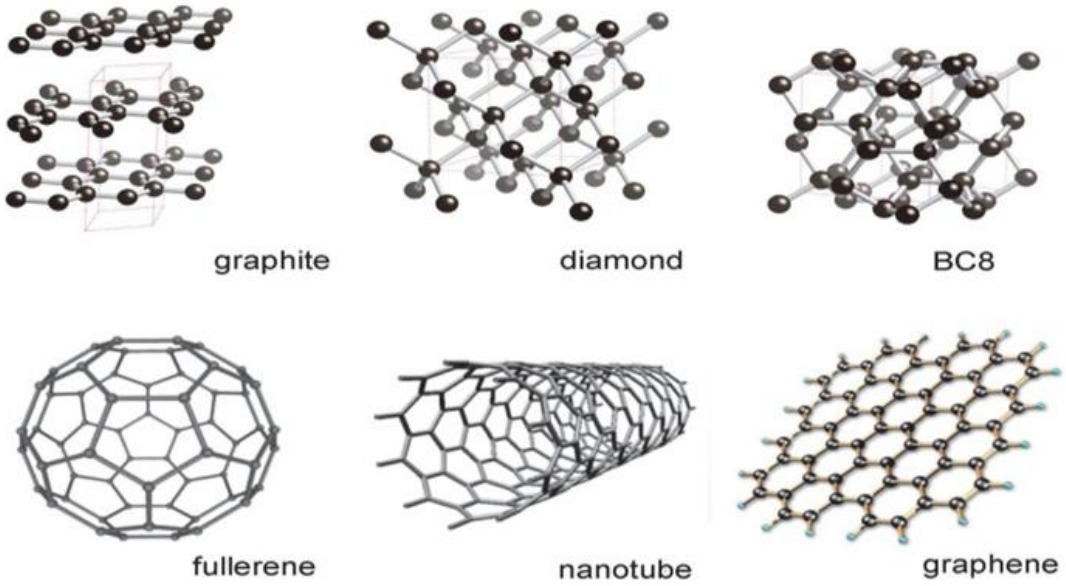

Figure 1: Allotropes of carbon [22]

Previously it is considered that elemental carbon exists only in two natural forms, graphite and diamond having extended networks of sp^2 and sp^3 hybridized carbon atoms bonded together respectively. Both show variable physical properties like electrical conductivity, thermal conductivity and hardness. Graphite and diamond known as the only form of carbon for a long time until carbon fibres were discovered in 1950's [5]. After which the research work carried out by scientists like Harold Kroto, Robert Curl, and Richard Smalley, who all win Nobel Prize in Chemistry in the year 1996 for the discovery of buckminsterfullerene in 1985. Fullerenes constitute the third allotrope of carbon [6]. Fullerenes are quite similar to that of sheet structure of graphite the only difference is they contain pentagonal rings which prevent sheet from planar structure. Fullerenes can be defined as a closed, aromatic and hollow carbon compound which is made up of twelve pentagonal faces and different numbers of hexagonal faces [7]. The discovery of fullerene initiates the beginning of synthetic carbon allotropes [1]. After which Iijima et al discovered carbon nanotubes in 1991 and graphene was discovered in 2004 by Geim and Novosolev. Due to numerous possible applications of

these allotropes, CNTs and graphene become an active research topic and large number of research is being carried out to explore them. The last two decades are marked by the research and development of nanostructure carbon materials and the interest which is generated in the scientific community is only because of carbon materials unique properties. Graphene, nanotubes and fullerenes are all based on the same structural unit that is a single layer graphene sheet which is left flat, rolled or wrapped. Carbon nanotubes are the only synthetic allotrope of carbon to reach large-scale industrial production [2].

Carbon Nanotubes

In 1990, S.Iijima and his group of NEC Laboratory in Japan succeeded in the creation of multi walled nanotubes by arc discharge method, which was previously used to synthesise fullerene [8]. After two years; they made the observation of single walled nanotubes. Carbon nanotubes are carbon allotropes having cylindrical nano structure. The atomic bonding of nanotubes is made entirely of sp^2 bonds, similar to bonds of graphite. This bonding structure, stronger than the sp^3 bonds of diamonds, give carbon molecules their unique strength.

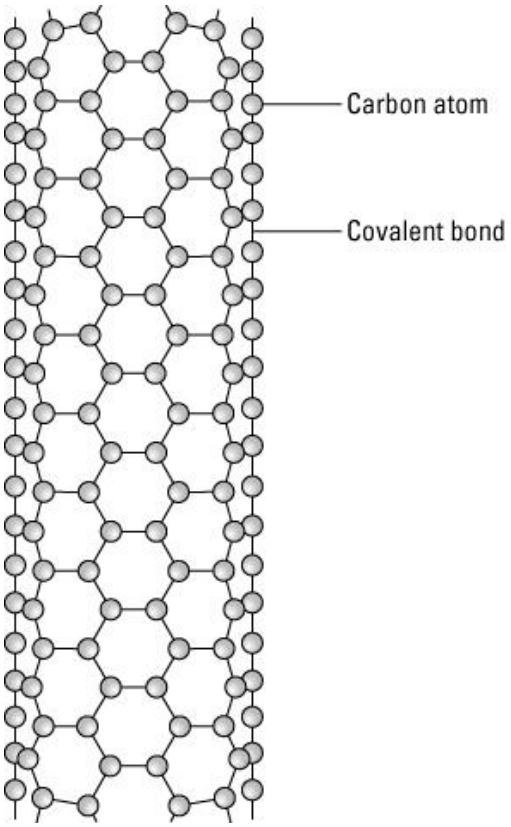

Figure 2: Carbon nanotube molecular structure [23]

Carbon nanotubes can be realise as a single atom thick graphene sheet which is rolled into tubular form [9]. These tubes have distinguished properties due to which they successfully achieve a wide research status throughout the world in recent times.

CNTs are one dimensional carbon structure. CNTs have tubular structure made up of carbon and having diameter in nanometres. One-billionth of a meter is a nanometre, and about ten thousandth of the thickness of a human hair. CNTs have many variations, differing in length, diameter, number of walls and type of chirality. CNTs have shown unique combination of tenacity, strength, and stiffness compared to the other fibres which mostly lack one or more of these properties. CNTs are having electrical conductivity and thermal conductivity very high as compared to the other conductive materials. CNTs have attracted interest for their unusual electrical properties making them best building blocks for nanoelectronics, nanosensors.

Types of CNTs

On the basis of walls

Single Wall Nanotubes (SWNTs)

SWNTs formation can be realise as wrapping single sheet of graphene into tubular form. SWNT could have diameter in between 0.4 nm - 2 nm. The structural properties of SWNTs have made them best material for the fabrication of nanotechnology based electronic devices. Their electrical conductance is comparable to that of copper having current densities up to 1013 A/cm^2 and a resistivity around 0.34 x 10^{-4} Ω.cm at room temperatures and thermal conductivity (3000 - 6000 W.m/K) [19]. SWNTs adsorb environmental gases which affects the conductance of a tube, and the presence of metal affects the electronic properties of SWNTs.

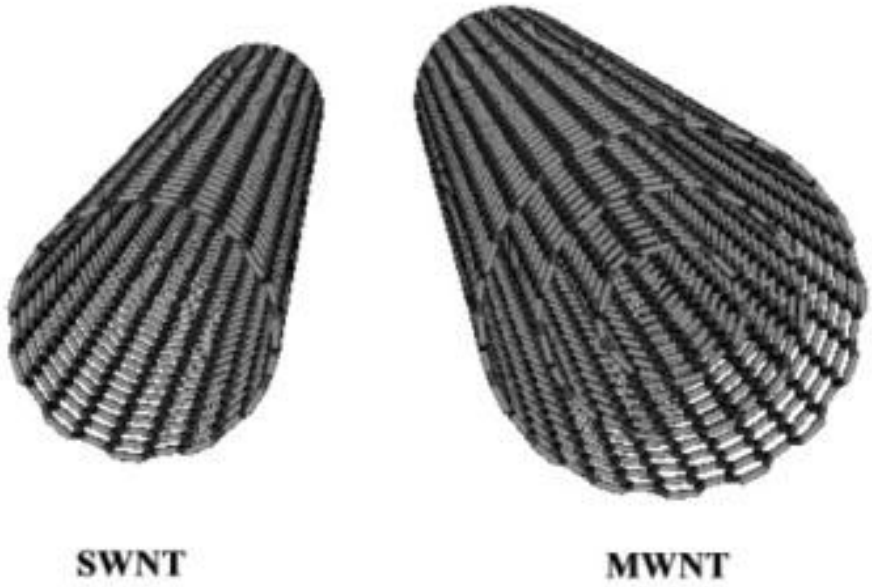

Figure 3: Types of CNTs on the basis of no. of walls [24]

Multiwall Carbon Nanotubes (MWNTs)

MWNTs are composed of several co-axial SWNTs one inside the other. They have been used for producing high strength composites. Multi-walled carbon nanotubes can be used to prepare natural rubber, nano-composites [3]. MWNTs are easy to synthesise in high volume quantities as compare to SWNTs. The structure of MWNT is less understood due to its greater complexity. Arc discharge method is best to produce high quantity MWNTs.

On the basis of chirality

SWCNTs form different orientations, which can be described using chiral vector (n, m), for vector equation $R = n_{a1} + m_{a2}$ where n and m are integers. Imagine that the nanotube is unravelled into planar sheet. The axis of the tube can be defined along the two parallel lines. When rolled, these parallel lines meet specifying the closing of tube along the length.

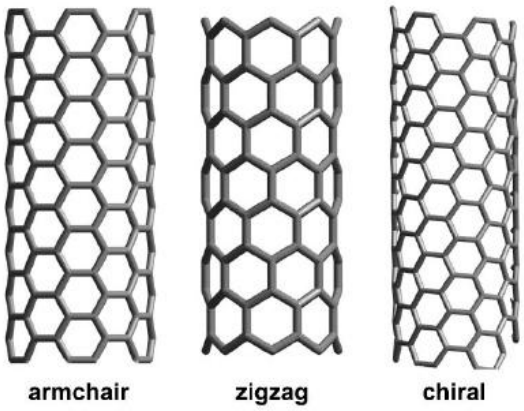

Figure 4: Types of CNTs on the basis of chirality [25]

Chirality depends on the axes of rotation of graphene sheet to realise a CNTs. The chiral angle which is used to differentiate carbon nanotubes into different classes by their electronic properties or band gape variations, they are:

• Armchair ($n = m$, $\theta = 30°$)

• Zigzag ($m = 0$, $n > 0$, $\theta = 0°$)

• Chiral ($0 < |m| < n$, $0 < \theta < 30°$)

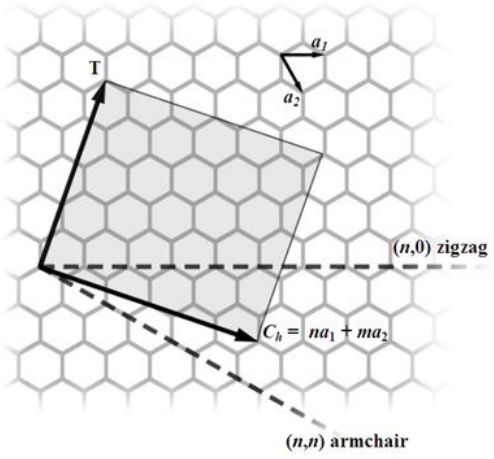

Figure 5: Chirality axis of rotation for CNTs [25]

Armchair carbon nanotubes have zero band gap making them metallic. Zigzag and chiral nanotubes can be metals having a finite band gap when $(n - m)/3$ = integer and $m \neq n$ or semiconductors in all other cases. The band gap for metallic and semiconductor nanotubes depends on tube diameter, which gives each nanotube a unique electronic property.

Properties of Carbon Nanotubes

Carbon is a unique element which can form one, two, or threefold strong chemical bonds. Graphene is a planar threefold configuration of carbon atom which when mould into a tubular geometry, carbon nanotubes can be realise. Properties of carbon nanotubes may change properties depending on whether SWNTs or MWNTs are taken into consideration [4]. Nanotubes are nanomaterial which have diameter in the molecular dimension and length may be macroscopic scale. CNTs chemical and physical behaviour are governed by their different structural features. They are stable till 750 °C in air atmosphere but are damaged after 750 °C due to oxidation mechanism and are stable till 1500 - 1800 °C in inert atmosphere after this temperature they become regular polyaromatic solids.

Electrical properties:

Nanotubes can be metallic or semiconducting depends on their chiral vector. For a (n,m) nanotube, if n=m, CNTs are metallic; if n-m is a multiple of 3, CNTs are semiconducting with a very low band gap, or else CNTs are a moderate semiconductor. That's why all armchair nanotubes are metallic as (n=m), and nanotubes other than that are semiconducting. SWNT's are characterized as ballistic conductors because of their geometry. They are one dimensional conductor with flow of electrons in single direction with no backtracking. Unlike MWNT, consisting of several concentric SWNT, they are not considered as 1D conductor. Here, the electron is not confined to one shell. In ballistic conditions, the electrical resistivity of SWNTs and MWNTs is very low such that these can prove to be better conductors than metals like copper. In ballistic conditions, SWNT: 10^{-6} Ωcm MWNT: 3×10^{-5} Ωcm [19].

Mechanical properties:

CNTs are the strongest and stiffest materials. Tensile strength and elastic modulus is quite high in CNTs as compared to steel. This strength results from the covalent sp^2 bonds formed between the individual carbon atoms. Tensile strength is between 11-63 Gpa and Young's Modulus is between 270-950 GPa [19].

Thermal Conductivity:

They are one of the best heat conducting materials. Ultra small SWNT's have been shown to exhibit superconductivity below 20K. They are also very stable at high temperature and also against strong acid because of their perfect conjugated system. The thermal conductivity of CNTs (room temperature) is 2000 W/m K and its 5 times greater than copper (400W/m K) [19].

SYNTHESIS OF CARBON NANOTUBES

CNT Growth Techniques

CNTs can be grown by lots of different methods under different conditions [10]. Some of them are used worldwide for CNTs growth which has been discussed briefly below. The type of CNT growth whether SWNTs or MWNTs can differ depending on the type of method and conditions used.

Arc discharge method

The setup of this method consists of a vacuum chamber with two carbon electrodes in it. Carbon electrodes serve as the carbon source for the formation of CNTs. An Inert gas is fed (like He, Ar) into the chamber which enhances the speed of carbon nanotube formation. High voltage dc is passed between the anode and cathode which creates plasma of inert gases in space between the two electrodes. This plasma evaporates carbon atoms from the carbon electrodes and then deposited on the negative electrode for the nanotube formation. The yield and morphology of the CNTs is dependent on the atmosphere in which arc discharge is made [11]. The high yield of CNT could be attained on the basis of uniformity of plasma arc and the temperature conditions. This method yields up to 30% pure cnts. It can produce both SWNTs and MWNTs but with few structural defects and random sizes.

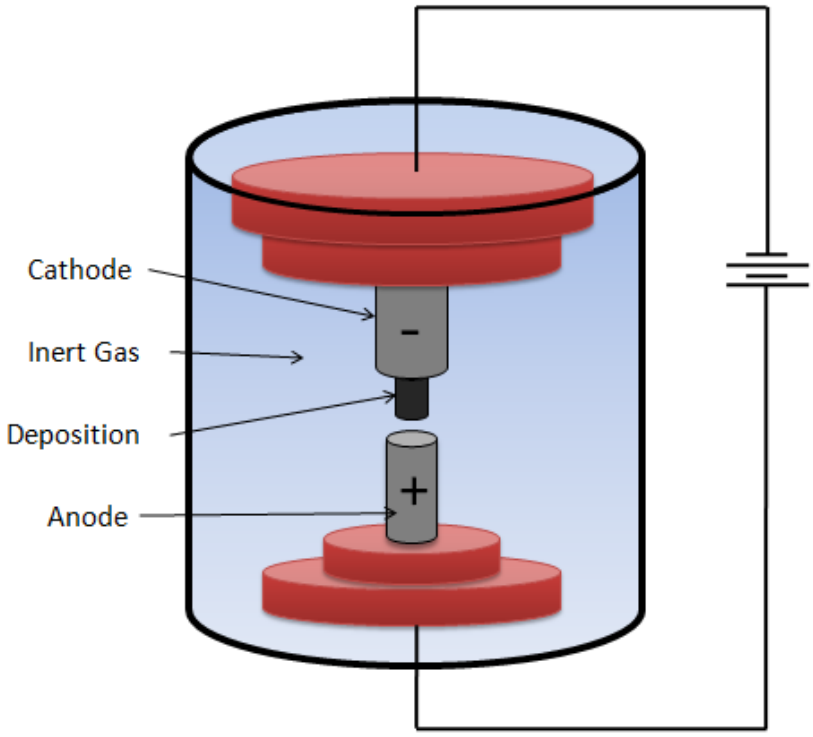

Figure 6: Schematic diagram of arc discharge method [26]

Laser Ablation method

This method for CNT growth was originated in year 1995 and was originally used for the production of metal Nano particles. In this method of the CNT production a graphite target is evaporated using pulse laser, in the presence of suitable catalyst like Co/Ni. Soot is generated due to the heating of graphite by the laser beam and from this soot CNTs are generated on the cold cathode [12,13]. The laser source can be a pulse laser [14, 15] source or it can be a continuous laser source. The main difference between the two is that for continues laser source we require a low intensity laser source and for a pulse laser source a high intensity laser source is required. The first large-scale production of SWCNTs was conducted in 1996 by the Smalley group at Rice University [16]. The laser ablation technique uses a 98.8% of graphite with 1.2% of cobalt/nickel composite target which is placed in a 1200 °C tubular furnace with an inert gas atmosphere of Ar/He, at ~500 Torre and target vaporize with a laser pulse. Nano scale metal catalyst particles are formed in the vaporized graphite plume. The growth of SWCNTs catalyse by these metal particles in the plasma plume, and also many by-products forms in this process. The nanotubes and by-products get collected through condensation on a cold finger downstream from the target inside chamber. SWCNTs yield varies from 20 to 80% by weight. The diameter distribution of SWCNTs achievable by this method is between 1.0 and 1.6 nm.

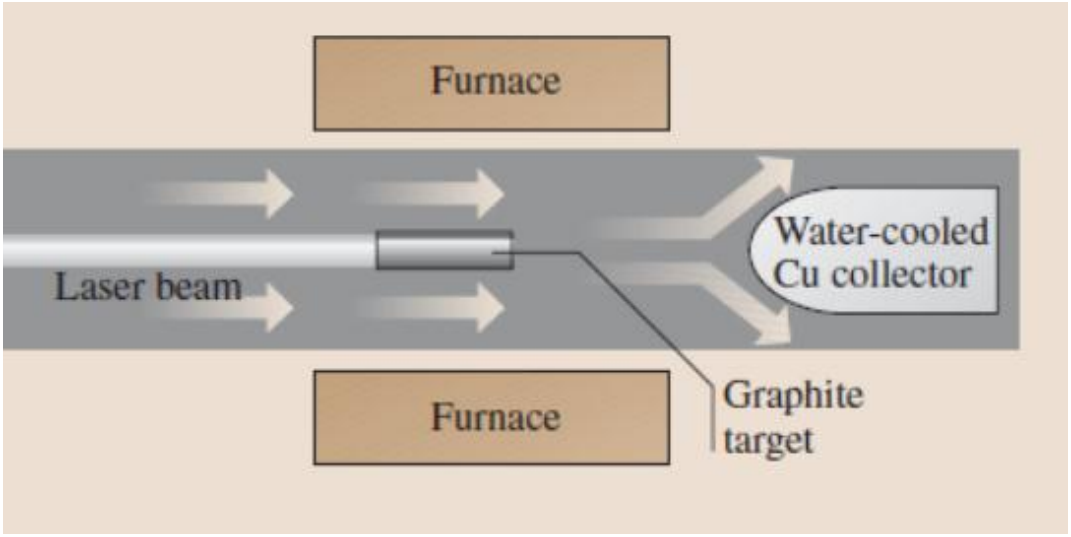

Figure 7: Schematic diagram of laser ablation method [27]

Thermal Chemical Vapour Deposition (T-CVD)

The T-CVD method is a controlled process for the selective synthesis of CNTs either in the bulk or in low amount [17]. T-CVD is the process where carbon precursors and carrier gas in vapour phase are transported to the reaction chamber where they get decomposed on the surface of the catalyst particles due to high temperature. The T-CVD method allows the CNT growth at much lower temperatures compared to the arc discharge and laser ablation methods. The carbon sources generally used are (C_2H_2, CH_4, C_2H_4, etc.). T-CVD reactor consists of quartz tube and the sides are used for the flow of different gases. The controlled flow of gases, their types and the temperature is generally optimized for the growth of CNTs. Chemical vapour deposition this term is used to represent heterogeneous reactions in which solid products are grown from one or two volatile precursors through chemical reactions, and these solid products get deposited on a substrate inside the T-CVD reactor. Transition metals like nickel, cobalt and iron are used as catalysts because of their high carbon solubility into them, carbon get defuse inside these metal partials [17, 18].

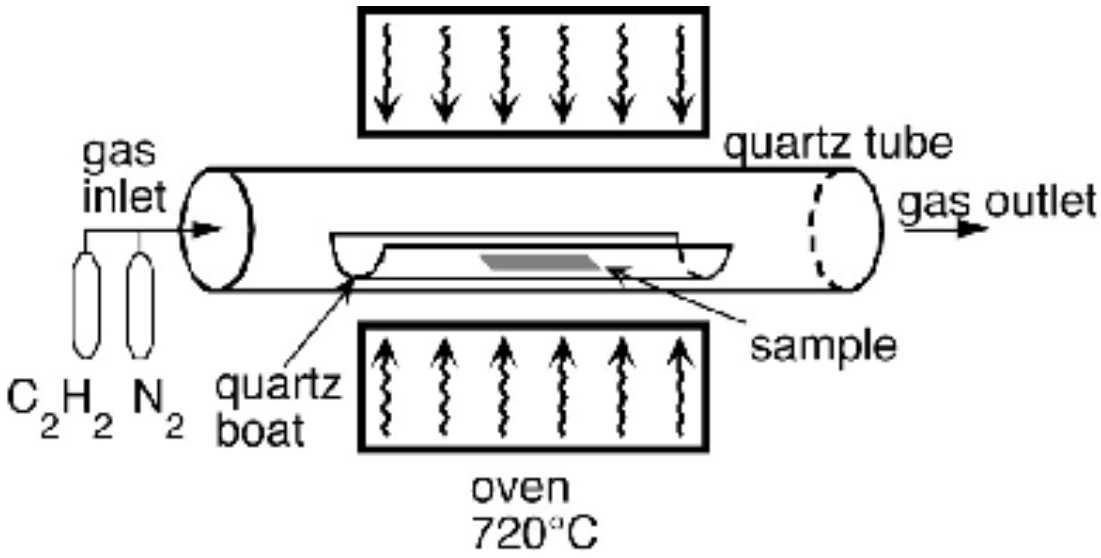

Figure 8: Schematic diagram of thermal chemical vapour deposition [28]

Plasma enhanced chemical vapour deposition (PECVD)

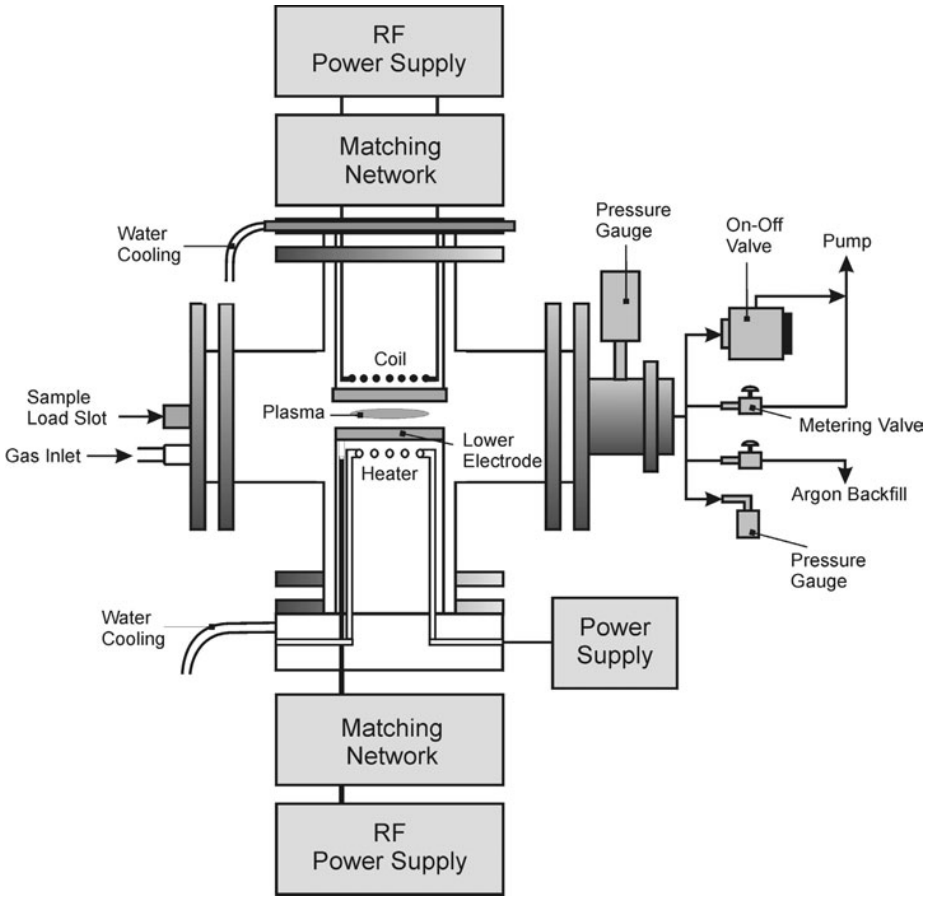

Figure 9: Carbon nanotube growth by PECVD: a review [21]

Plasma-enhanced chemical vapor deposition (PECVD) is a process in which thin films of desired material from a gas state (vapor) precursor is deposit on a substrate as solid state product. When plasma is produce, chemical reaction between the two or more gases will take place. Plasma is generally created between two electrodes by RF frequency or DC voltage discharge. When high frequency voltage is applied between two electrodes a glow discharge of precursor gases take place inside the reaction chamber. The substrate is placed on the grounded electrode and the reaction gas is supplied from the opposite side of the substrate. We use catalyst such as Fe, Ni and Co nano particles for carbon nanotubes growth on these metal particles formed by glow discharge on the substrate, generated by high DC voltage or RF voltage. A reaction gas that contains carbon such as CO, C_2H_2, C_2H_6, C_2H_4, or CH_4 is introduced into the chamber. The catalyst conducts a very important role on carbon nanotubes diameter, growth rate, wall thickness and morphology.

Chapter-2 LITERATURE REVIEW

Several procedures have been proposed in literature for direct growth of MWCNTs on stainless steel by chemical vapor deposition and their applications. In this section, first of all some of these techniques are explained which are implemented to compare the performance of proposed procedure.

Growth of carbon nanotube by thermal CVD method on stainless steel 304 without addition of any external catalyst [30]

In this research paper author discussed a method to synthesize carbon nanotubes (CNTs) by thermal CVD directly on stainless steel substrates. Bulk steel surface act as a catalyst and support substrate for the CNT growth, due to which adhesion between substrate and CNTs is very high. This group synthesise CNTs at different growth temperature and different HCl pre-treatment time. A general growth procedure they follow is as following

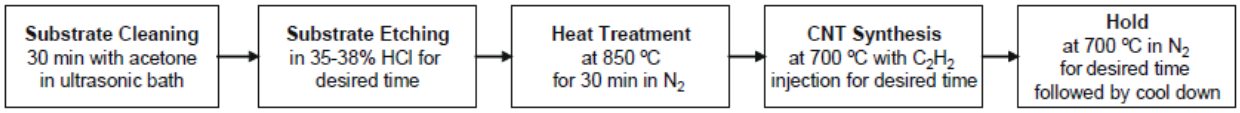

Figure 10: Procedure for CNT growth on SS 304 by [30]

Author concluded that they were able to produce a thin layer of CNT on stainless steel 304 which is uniformly grown. Some of their result SEM images are as following which shows a uniform growth of CNTs on SS 304.

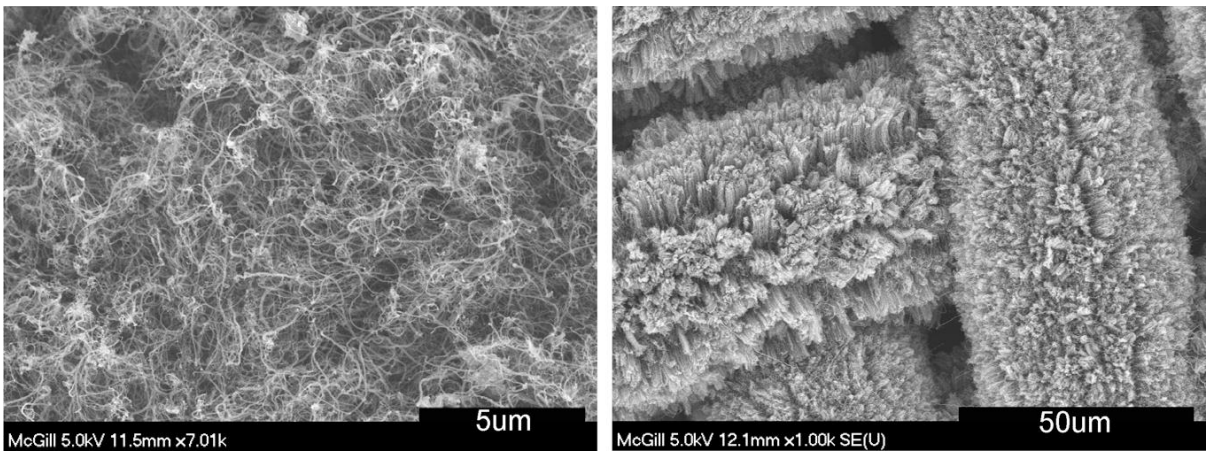

Figure 11: SEM micrograph of CNTs on SS grid at different magnifications [30]

Stainless steel mesh coated with carbon nanotube application in biocathode microbial fuel cells [31]

In this research paper author fabricates carbon nanotubes coated stainless steel mesh (SSM) electrode fabricated by dipping SSM in CNTs ink and they used this as biocathode in microbial fuel cell (MFC), they got improved performance. SEM images shows that CNTs are uniformly spread on the surface of the SSM, which is forming a three-dimensional network structure of large surface area.

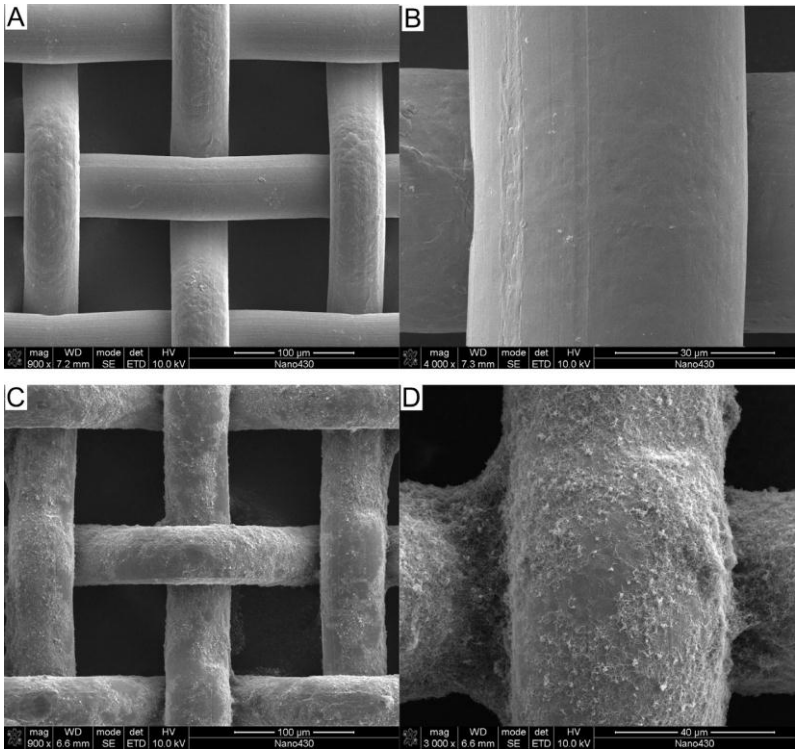

Figure 12: SEM micrograph of abiotic biocathodes. Image A, B are of bare stainless steel mesh and C, D are of CNTs coated stainless steel mesh [31]

They observed that the MFC with CNTs coated SSM biocathode shows higher Columbic Efficiency than MFC without CNTs coated SSM biocathode. Author concluded that CNTs coated SSM offers an effective way to enhance the electricity of biocathode microbial fuel cell.

Dependence of CNTs diameter on interwall separation and strain probed by X-ray diffraction and Raman scattering studies [32]

In this research paper author done a study on diameter dependent spectral features in Raman scattering and X-ray diffraction of MWCNTs of different diameters (5−100 nm). HRTEM imaging shows a systematic decrease in the interwall separation as the diameter of MWCNTs increases.

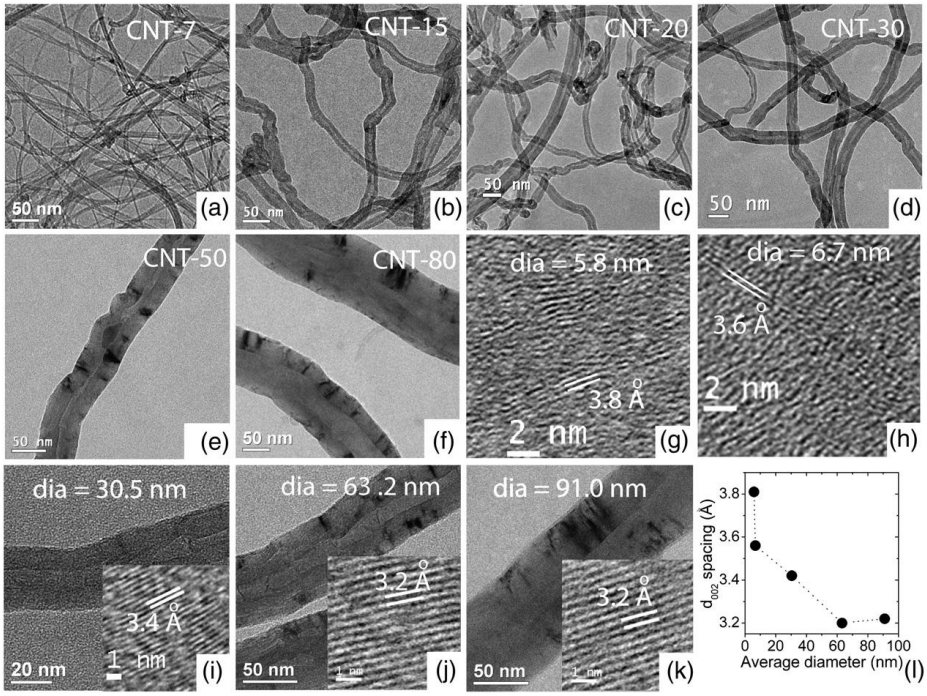

Figure 13: HRTEM images of different diameter MWCNTs (a) 7 nm, (b) 15 nm, (c) 20 nm, (d) 30 nm, (e) 50 nm and (f) 80 nm. CNTs lattice spacing and diameter (D) is shown in: (g) 3.8 Å, D=5.8 nm, (h) 3.6 Å, D=6.7 nm (i) 3.4, D=30.5 nm, (j) 3.2 Å, D=63.2 nm, (k) 3.2 Å, D=91 nm. (l) Variation of lattice spacing with diameter of MWCNTs is shown. [32]

Author concluded by Raman and XRD data that the lowest or 7 nm diameter MWCNTs have features similar to that of SWCNTs. And the spectral features are quite different for higher diameter MWCNTs due to the interaction between tube walls.

Growth of MWCNTs on stainless steel 316 by CVD and study of effect of surface nano features on CNT growth [33]

In this research paper auther synthesise MWCNTs by chemical vapour deposition directly on asreceived and pretreated SS 316 substrate without application of an external catalyst. The size distribution of surface features with respect of different steps of the synthesis process were described which show that the heating cycle and any pre-treatment may produce significant changes of the surface morphology, with this they conclude that any initial characteristics of the as received surface or any caused by a pre-treatment, will occur in conjunction with the heating effect. Average size of nano-features less than 60 nm were observed which were responsible mainly for the CNTs growth and a larger features size was associated to the carbon nanofiber synthesis. SEM Images of HCl treated substrates are as following.

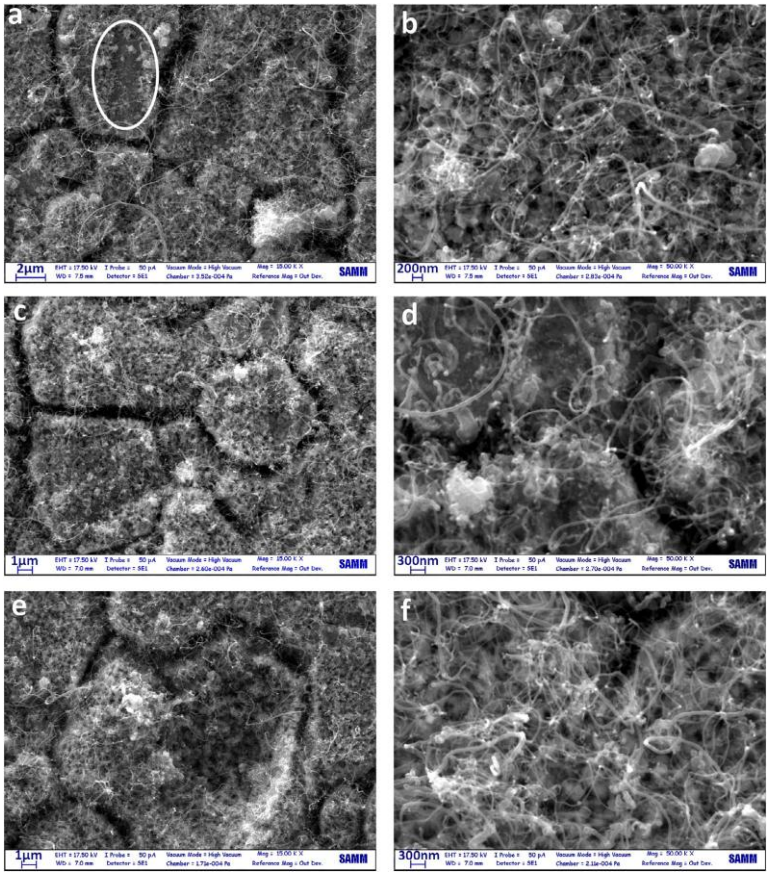

Figure 14: SEM micrographs of samples with 5 min HCl and 10 min growth time (a and b), 5 min HCl and 20 min growth time (c and d) and 10 min HCl and 20 min growth time (e and f) in different magnifications. [33]

Synthesis of carbon nanotubes directly on stainless steel to use as electrode in a glucose fuel cell [34]

In this research paper author synthesise MWCNTs directly on the surfaces of stainless steel mesh by oxidation followed by reduction treatment with a carbon source of ethylene-hydrogen gas mixture, and this mesh was used in a glucose fuel cell as anode. After MWCNTs synthesis author dispersed Pt nanoparticles on it by magnetron sputtering. They observed power generation efficiency of Pt per unit mass became 33 W/g. They found this method of CNTs synthesis is very suitable for fuel cell electrode as by this method CNTs can be grown on complicated electrode structures. Structure of the glucose fuel cell used in this research work is as following

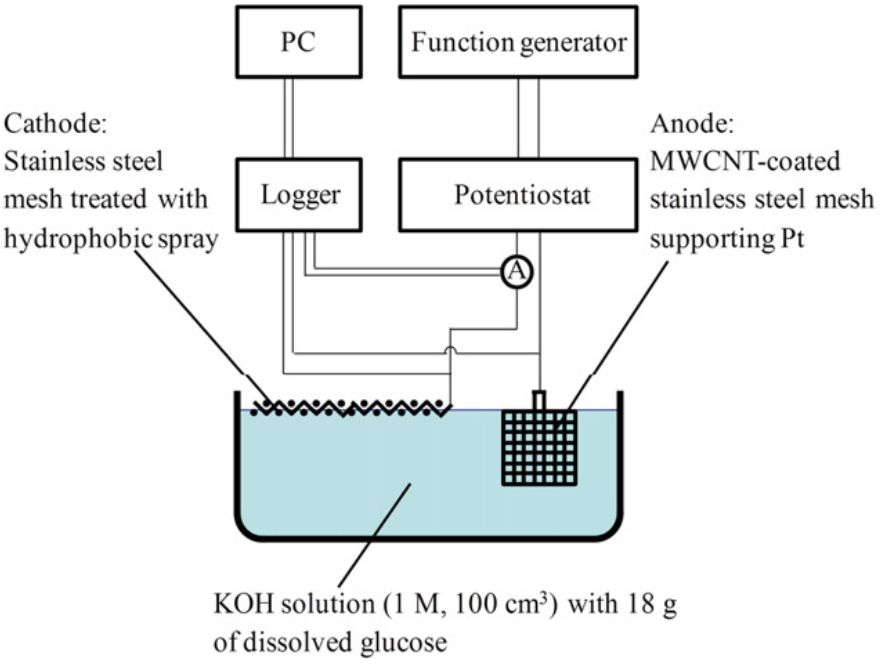

Figure 15: Structure of the glucose fuel cell constructed for this work [34]

Direct growth of carbon nanotubes and nanofibers by CVD and its effect on nanostructure and electrochemical corrosion behaviour of stainless steel 316 [35]

In this research paper author investigated corrosion behaviour of three differently treated SS 316 plates. Which are pristine, CNTs coated SS 316 and carbon nanofiber (CNF) coated SS 316. CNTs and CNFs were directly grown on stainless steel by CVD method, they use ethylene as the carbon source. They investigate corrosion behaviour of this samples by a combination of microstructural and electrochemical methods. Electrochemical tests included potentiodynamic and potentiostatic techniques in hot sulfuric acid solutions. They observed strong deterioration in corrosion resistance by the electrochemical tests, which they confirmed by microstructural examination of the samples. They found that carbon diffusion into SS 316 substrate during the CNT/CNF growth process results in chromium depletion of the near-surface region of SS 316 and chromium carbide precipitation at grain boundaries causing accelerated intergranular corrosion. SEM image of CNTs and CNFs are as following

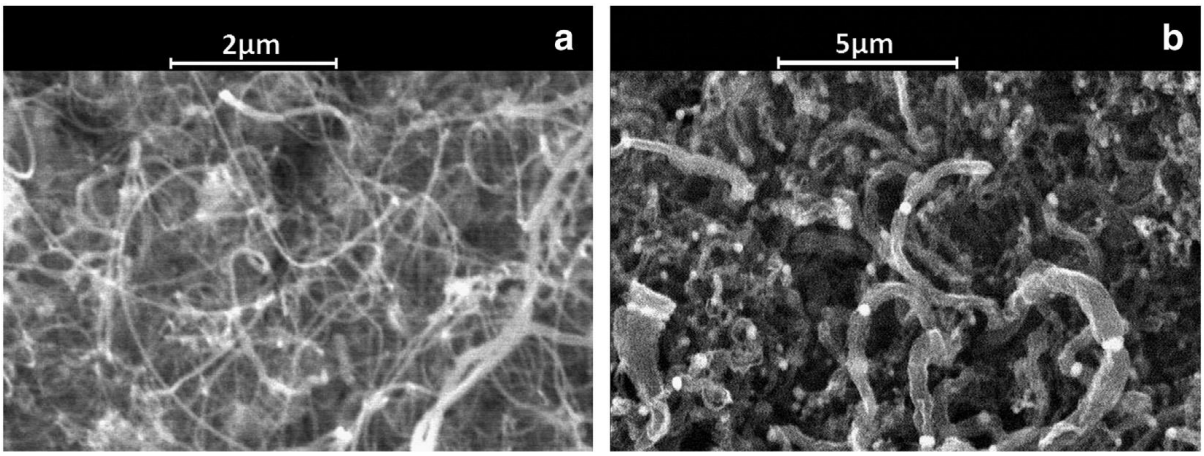

Figure 16: SEM micrographs showing (a) CNTs (b) CNFs [35]

Study of carbon input on the morphology and attachment of CNTs synthesised directly on stainless steel [36]

In this research paper author synthesise multi-walled carbon nanotubes by CVD directly on SS 316 mesh without any pre-treatment or use of any external catalyst. They introduce a growth method in which particle like growth sites were generated, which were created due to chromium migration from the bulk to the surface of substrate during heating. Author shows that by varying acetylene concentrations and growth time diameter of CNTs is changed. They also observed that CNTs produced were rooted strongly to the SS 316 substrate. Larger diameter CNTs were much more difficult to break or remove by ultrasonication then smaller size CNTs. SEM image of CNTs growth with different growth time is shown below; more the growth time larger will be the diameter of CNTs

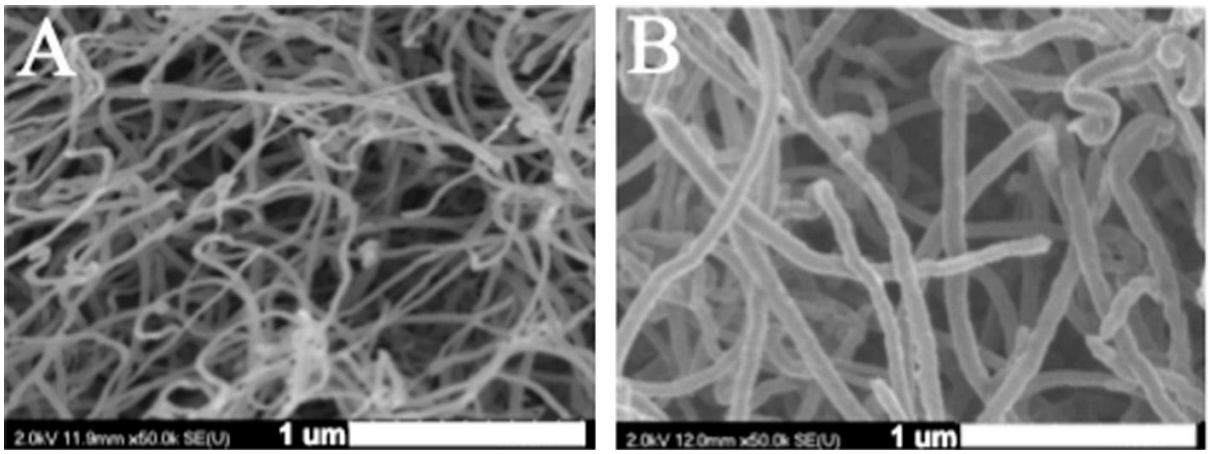

Figure 17: SEM micrograph of CNTs at various C_2H_2 injection durations is shown. (A) 1 min, (B) 30 min, both case C_2H_2 flow rate 45 sccm [36]

Growth of carbon nanotubes on Ar ion bombarded stainless steel 304 substrates [37]

In this research paper author synthesise Carbon nanotubes on Ar ion bombarded SS 304 substrate directly by chemical vapor deposition, they use C_2H_2, NH_3 and H_2 as gas precursors at 800 °C of growth temperature. They use variable ion doses and energies in pre-treatment with H_2 and NH_3 at 750 °C. They investigated effects of ion energy and dose on the growth of CNTs according to which they found ion energy and dose both were modifying the grain structure and increase the roughness of the SS 304 substrate surface. AFM images of SS 304 substrate surface treated by Ar ions with a dose of 4×1018 ions/cm^2 at energies of 30 keV, 20 keV and 4 keV is as below

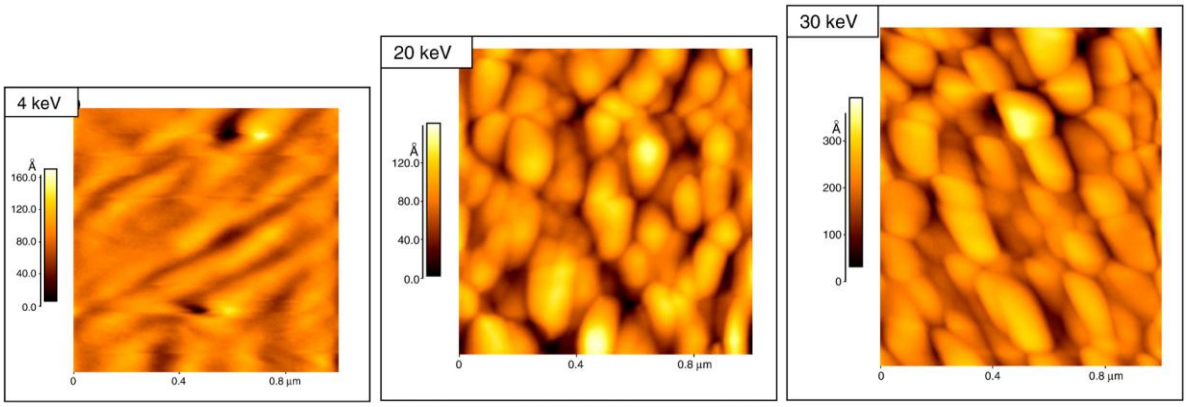

Figure 18: 2D AFM images of SS 304 substrate surface treated by Ar ions with a dose of 4×10^{18} ions/cm^2 at energies of 4, 20 and 30 keV respectively. [37]

Carbon nanotube synthesis on plasma pre-treated stainless steel 316 substrates. [38]

Author presented in this research paper direct growth of carbon nanotubes on SS 316L sheets without extra deposition of catalytic and buffer layers. They compared effects of substrate pre-treatment procedure consisting of a combination of Ar-plasma treatment and air annealing to introduce morphological changes on the substrate surface. They performed plasma treatments and air annealing by a cylindrical plasma chamber and thermal furnace respectively. They observed that roughness of the substrates got altered by growth temperature, annealing temperature and plasma pre-treatment. They conclude that the highest CNT height they achieved is of 23.5 μm on a substrate which was first prepared by Ar-plasma (30 min) and then by air annealing (10 min at 725 °C). TEM images of this pre-treatment are as below.

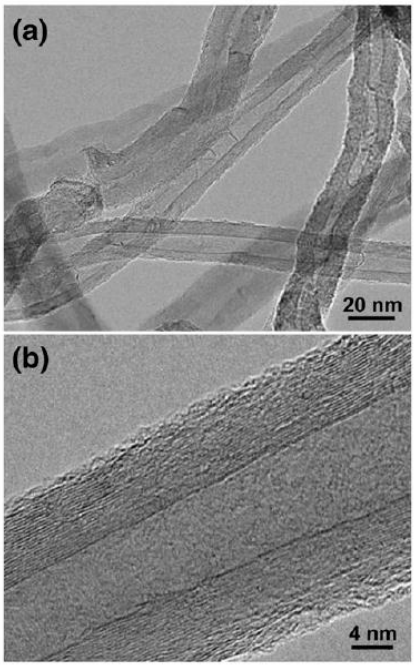

Figure 19: (a) TEM image of CNT grown using substrates which was first prepared by Ar-plasma (30 min under 10.5 W) and then by air annealing (10 min at 725 °C). (b) A magnified TEM image shows highly crystalline CNT structure. [38]

Synthesis of multi-walled carbon nanotubes in a porous stainless steel block [39]

In this research paper author synthesise high purity MWCNTs on the inner and outer surfaces of porous stainless steel block with each side equal to 1cm and having pores diameter of approx 300 µm. They activated inner surface of the stainless steel by oxidation in O_2-Ar at 800 °C and after that by reduction in H_2-Ar at 700 °C. After that they introduce a mixture of ethylene and Ar gases in the pores of SS block for the formation of the MWCNTs. The MWCNTs which they synthesise have uniform structure and purity throughout the entire stainless steel block. Optical image (on cm scale) and SEM image of the substrate are as below.

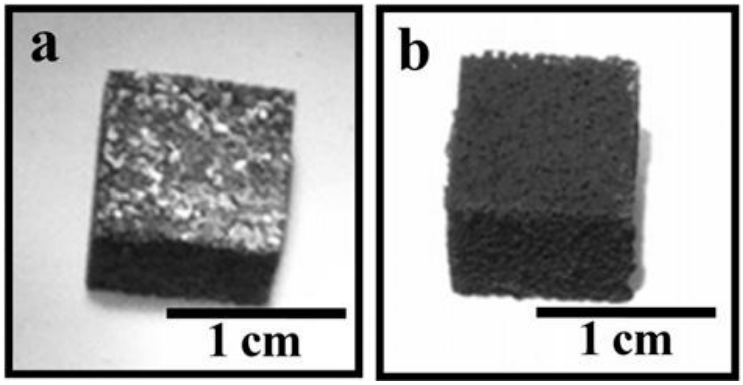

Figure 20: Optical image of (a) untreated porous stainless steel block and (b) MWCNTs synthesized on block. [39]

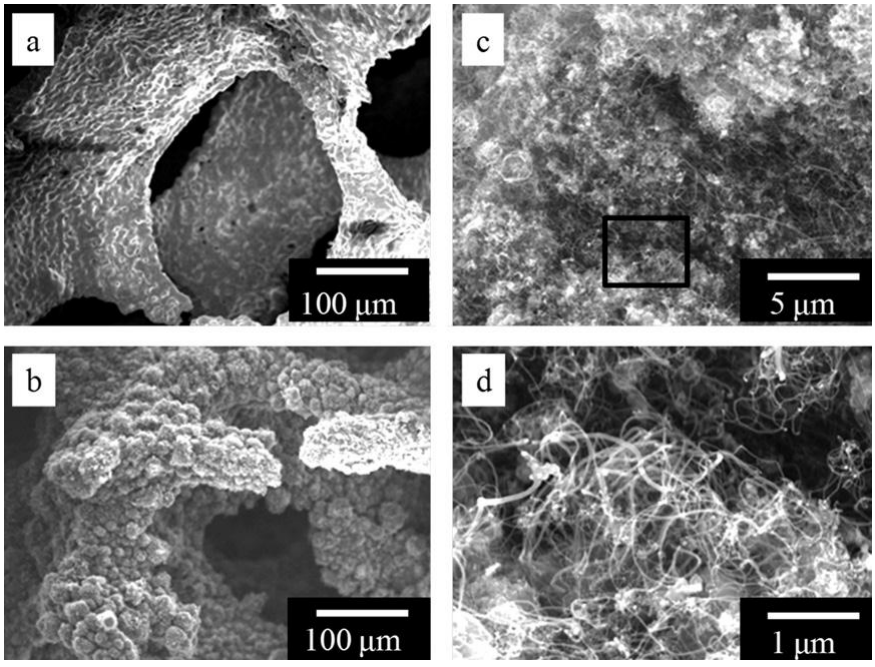

Figure 21: SEM micrograph of (a) untreated porous stainless steel block, (b, c, d) of the porous stainless steel block with MWCNTs synthesized on it in different magnification. [39]

Chapter-3

EXPERIMENTAL DETAILS

The Thermal-CVD Setup at DTU Nanotechnology Lab

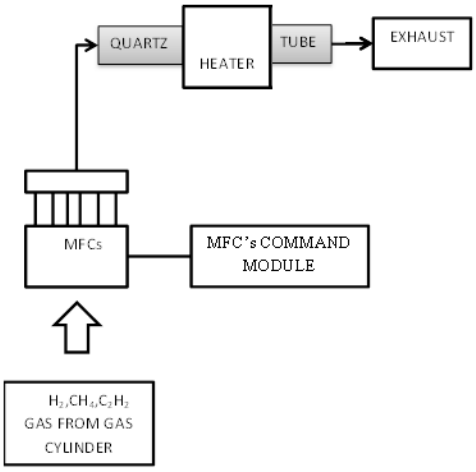

Figure 22: Block diagram of T-CVD setup at DTU Nanotechnology Lab

The T-CVD setup at DTU Nanotechnology Lab consists of

- A horizontal single zone tubular furnace having 5 cm of hot zone near to the centre of the furnace. Length of this furnace is 40 cm with an inner diameter of 6 cm where quartz tube is inserted. The maximum temperature it can reach is around 900 °C.
- Quartz tube is the main reaction chamber inside which Substrates are placed for CNTs growth. The dimensional parameters of Quartz Tube used here are 60 cm length, 4 cm outer diameter and 3.6 cm inner diameter.
- Command module is an instrument which serves as an interface between users and MFCs, to set a flow rate of gas we need to feed those values in it. Command module which we used is from MKS Instruments.
- Mass Flow Controllers (MFCs) is having a gas flow sensor, a gas flow control valve and an electronic circuit to maintain desired gas flow rate all build in one casing. MFCs are calibrated to control flow rate of a particular gas, we have MFCs of C_2H_2, Ar, H_2, CH_4 at DTU Nanotechnology Lab. These MFCs are also from MKS Instruments.
- Gas Cylinders of C_2H_2, Ar, H_2, CH_4 are there in DTU Nanotechnology Lab.

Figure 23: Photograph of T-CVD furnace.

Experimental Procedure

Substrate pre CVD Treatment

The Substrates used in this study were of Stainless Steel 304 with dimensions 10 mm X 10 mm X 1 mm. To make substrates a 2.5 cm X 70 cm X 0.1 cm Stainless Steel 304 bar (which we buy from local vendor, grinded with SiC abrasive paper of 500 grit) was cutted in workshop for desired dimensions using a shearing machine. The pre growth treatments processes on the above substrates are as following

1. Take 20 ml Acetone in a 100 ml beaker then dip all SS 304 substrates in acetone and sonicate them in Ultra sonicator for 10 minutes at 35 kHz. By this we clean substrates for further processing. Take these samples out and allow them to dry. Then designate these substrates as ‘‘acetone cleaned’’.
2. Take 20 ml concentrated HCl in 100 ml beaker then dip some acetone cleaned SS 304 substrate in HCl and sonicate them in Ultra sonicator for 10 minutes at 35 kHz. By this we etch substrate surface with more penetration depth inside the surface. Then designate these substrates as “HCl sonicated”.
3. Take 20 ml concentrated HCl in 100 ml beaker then dip some acetone cleaned SS 304 substrate in HCl for 10 minutes. By this we etch substrate surface with less penetration depth inside the surface. Then designate these substrates as “HCl dipped”.

Synthesis of Carbon Nanotubes

Synthesis of CNTs in this study includes two stages that is Heat treatment and Growth process. Heat treatment is done in Argon atmosphere at 800 °C. Growth process is done with C_2H_2 as carbon carrier gas at 800 °C. A process graph of CNTs synthesis is shown as below.

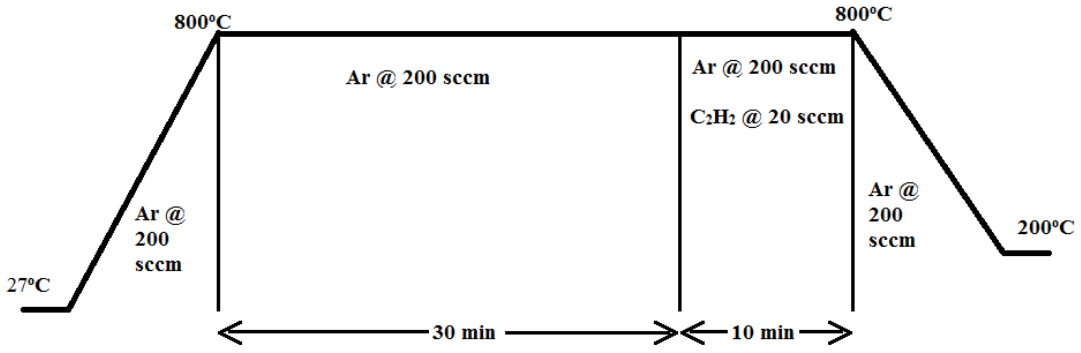

Figure 24: Systematic diagram depict process of CNTs synthesis

Detailed procedure is as following

1. Arrange the T-CVD setup as mentioned in the above session.
2. Take one substrate each from “HCl sonicated”, “HCl dipped” and “acetone cleaned”; then give them their sample name as “SS01”, “SS02” and “SS03” respectively. Total number of samples per run is three.
3. Take a quartz boat clean it properly with acetone.
4. Load the above three samples (“SS01-03”) on quartz boat.
5. Then load this quartz boat in the reaction chamber, such that all the substrates come under hot zone of the reaction chamber. Close the chamber openings.
6. Start flow of Ar at 200 sccm flow rate for 5 minutes.
7. Set furnace temperature controller at 800 °C and start heater. Furnace will take time to reach 800 °C; in this stage inner atmosphere of chamber is of Ar at 200 sccm.
8. When furnace temperature reaches 800 °C allow it to retain this temperature for 30 minutes in Ar atmosphere at 200 sccm. This is the heat treatment stage.
9. After this retain furnace temperature again at 800 °C for next 10 minutes, with Ar at 200 sccm and C_2H_2 at 20 sccm in the chamber. This is the growth process stage.
10. Then switch off Heater of the furnace, allow chamber to cool down in inert atmosphere of Ar at 200 sccm until chamber temperature reaches 200 °C.
11. Then open the chamber and unload it, put quartz boat on a safe table and unload samples from boat to sample box, mark properly sample name on sample boxes.

In this study two runes have been performed with the same procedures to get desired results, which are designated as “Run 1” and “Run 2” respectively. Sample names so assigned with their pre CVD treatments and after CVD treatment are as follow

Table 1: Samples details

Sample Name	Pre CVD Treatments	After CVD Treatment
“SS00”	As received without HCl treatment (For surface analysis)	No CVD Treatment
“SS01”	HCl sonicated for 10 min (For “Run 1”)	Amorphous carbon is there due to poor pre CVD treatments
“SS02”	HCl dipped 10 min (For “Run 1”)	Amorphous carbon is there due to poor pre CVD treatments
“SS03”	As received without HCl treatment (For “Run 1”)	CNTs were there but with very less coverage
“SS04”	HCl sonicated for 10 min (For “Run 2”)	CNTs were confirmed by SEM
“SS05”	HCl dipped 10 min (For “Run 2”)	CNTs were confirmed by SEM
“SS06”	As received without HCl treatment (For “Run 2”)	CNTs were confirmed by SEM
“SS07”	HCl sonicated for 10 min (For surface analysis)	No CVD Treatment
“SS08”	HCl dipped 10 min (For surface analysis)	No CVD Treatment

Characterization

Pre Treatment surface morphology and Deposited carbon layers were characterized by Atomic Force microscope (AFM) instrument, Scanning electron microscope (SEM), Energy dispersive X-ray (EDX).

Chapter-4 RESULTS AND DISCUSSION

Results

Results of each sample are as below

"SS00"

"SS00" is the as received SS 304 substrate grinded with SiC abrasive paper of 500 grit. Characterizations performed on this substrate were AFM, FESEM, EDX and XRD.

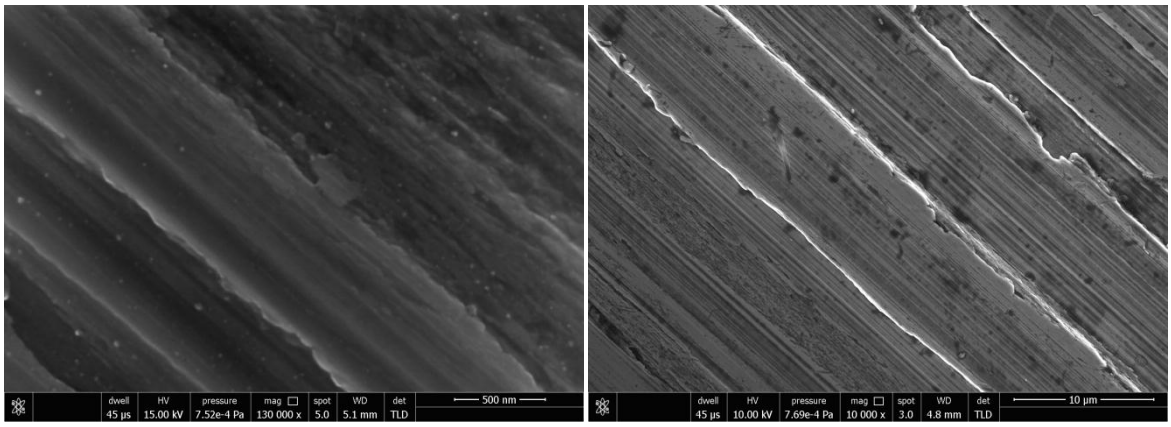

Figure 25: FESEM image of "SS00" (untreated) at different magnifications

FESEM images in Fig. 25 show the surface of SS 304 substrates which we used for pre-treatments and CNTs growth. In this image we can see some lined pattern which is due to grinding of substrate surface with SiC abrasive paper of 500 grit; even at 130000x magnification (500 nm scale) we can see some uniform lines. From AFM images in Fig. 26 we can see 3D view of the surface of the substrate. Roughness calculated by AFM (Ra) for 25 µm scale image is 109 nm and for 2 µm image is 5.19 nm.

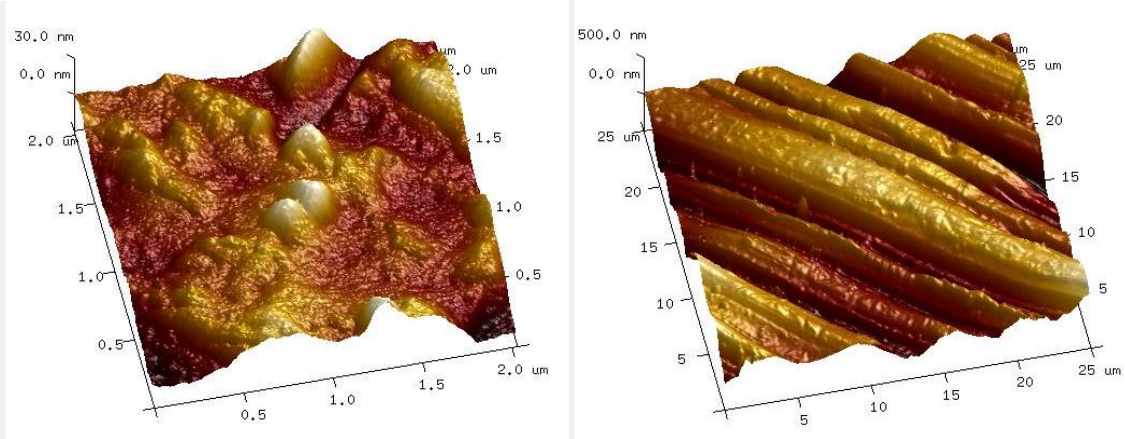

Figure 26: 3D AFM image of "SS00" (untreated) at different scales

Table 2: EDX data of "SS00" (untreated) substrate

Elements	Composition by Weight %
C	3.24
N	1.89
Cr	16.24
Mn	1.93
Fe	68.92
Ni	7.44

Elemental composition we got from EDX of "SS00" (untreated) substrate is almost same to the standard composition of SS 304 which is 18% Cr, 2% Mn, 8% Ni. The only difference is in the composition of carbon which should be around 0.1%; this deviation in from standard data can be due to surface contamination by atmosphere. Elemental compositions by weight have tabulated in Table 2 and EDX spectrum is shown in Fig.27.

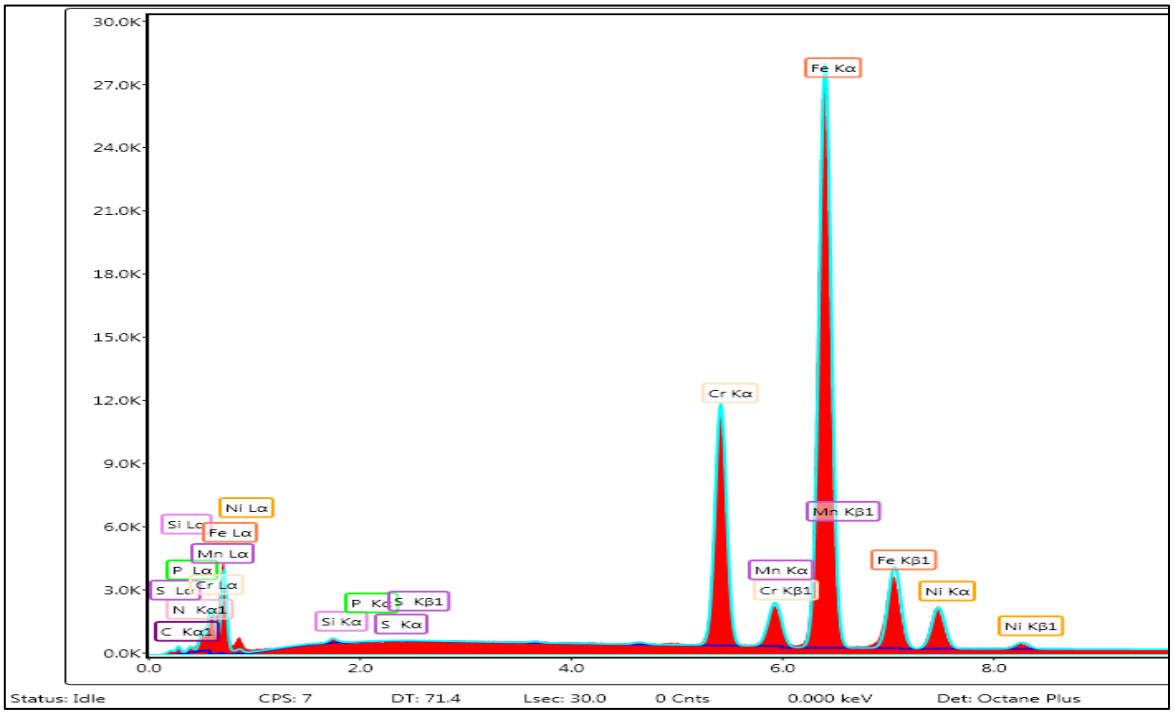

Figure 27: EDX spectrum of "SS00" (untreated)

“SS07”

“SS07” is the substrate of SS 304 which was sonicated in HCl for 10 min.

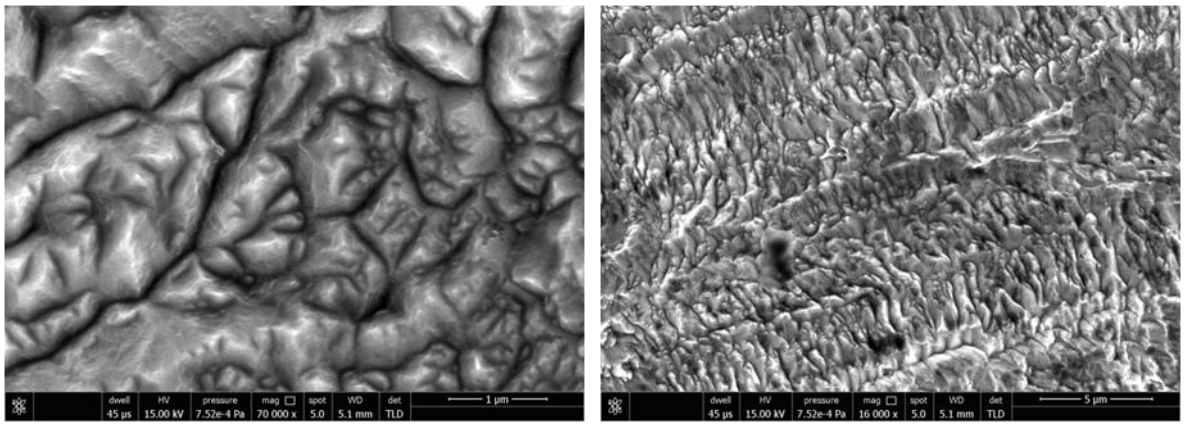

Figure 28: FESEM images of “SS07” (HCl sonicated) at different magnifications

FESEM images in Fig. 28 shows the surface of SS 304 substrates which is sonicated in HCl for 10 min to investigate pre CVD treatments. In this image we can see that polished SS 304 substrate gets etched by HCl removing a huge amount of surface materials of substrate and surface grain size is increased. From AFM images in Fig. 29 we can see 3D view of the surface of the substrate. Roughness calculated by AFM (Ra) for 25 µm scale image is 198 nm and for 2 µm scale image is 37.7 nm.

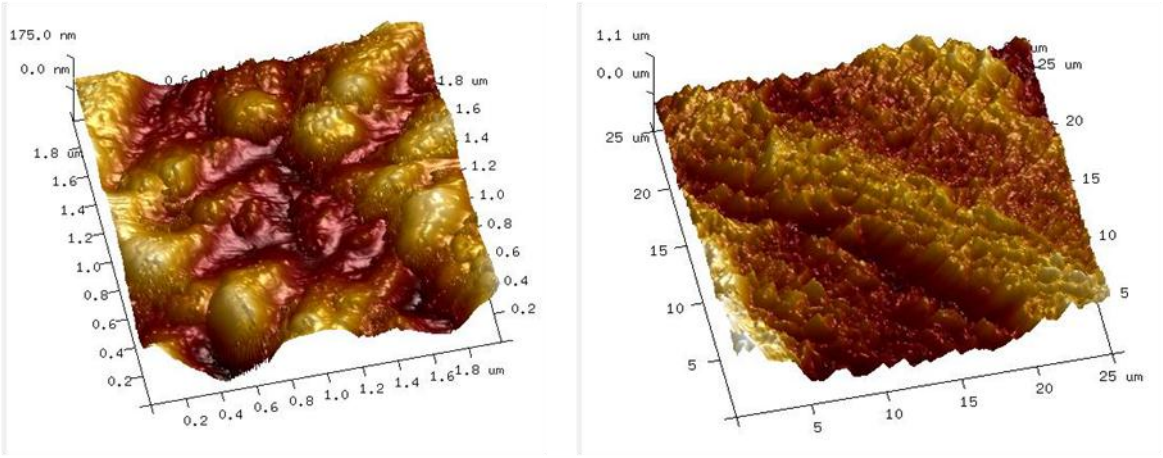

Figure 29: 3D AFM image of “SS07” (HCl sonicated) at different scales

Table 3: EDX data of "SS07" (HCl sonicated)

Elements	Composition by Weight %
C	3.51
N	0.75
Cr	16.76
Mn	2.13
Fe	69.64
Ni	7.01

Elemental composition we got from EDX of "SS07" (HCl sonicated) substrate is almost same to the "SS00" (untreated) substrate composition which is 16.24% Cr, 3.24% C, 7.44% Ni, 1.93% Mn. Elemental compositions by weight have tabulated in Table 3 and EDX spectrum is shown in Fig.30.

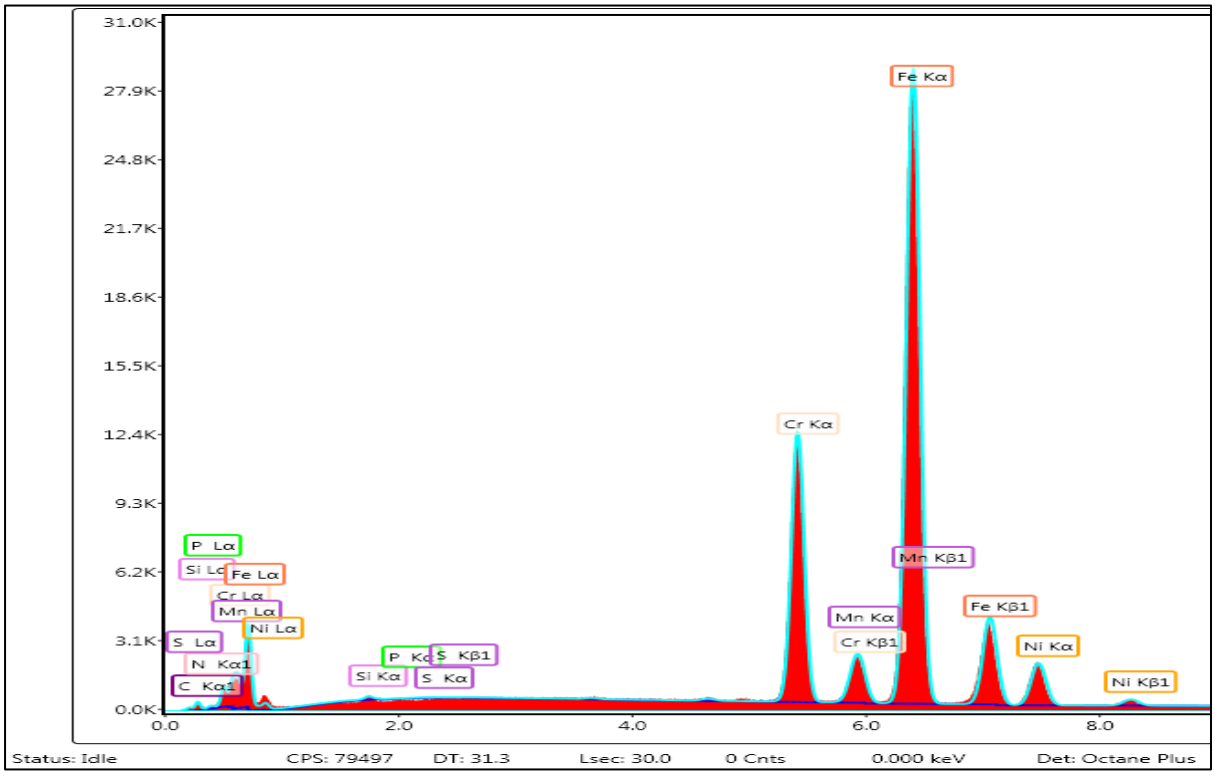

Figure 30: EDX spectrum of "SS07" (HCl sonicated)

“SS08”

“SS08” is the substrate of SS 304 which was dipped in HCl for 10 min.

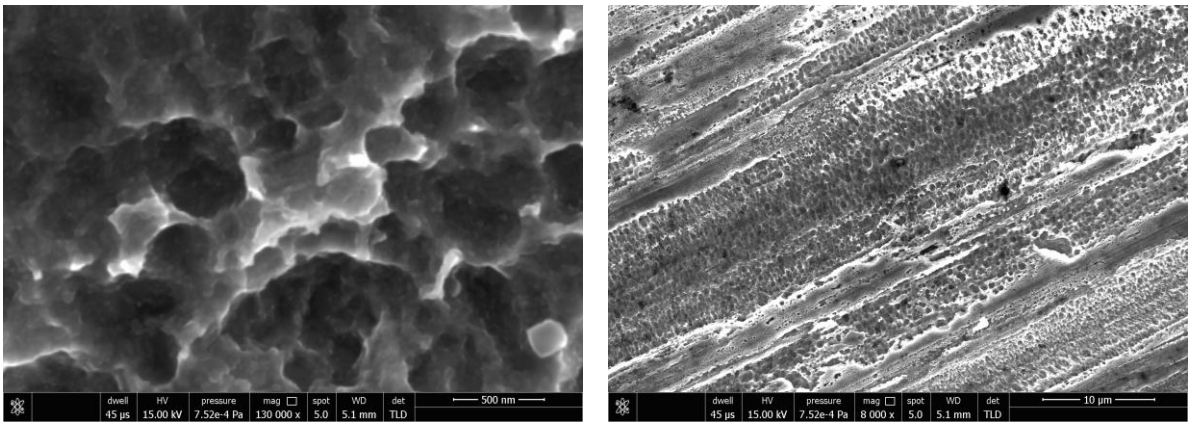

Figure 31: FESEM images of “SS07”(HCl dipped) at different magnifications

FESEM images in Fig. 31 shows the surface of SS 304 substrates which is dipped in HCl for 10 min to investigate pre CVD treatments. In this image we can see that polished SS 304 substrate get etch by HCl removing surface materials of substrate and making substrate surface porous. From AFM images in Fig. 32 we can see 3D view of the surface of the substrate. Roughness calculated by AFM (Ra) for 25 µm scale image is 252 nm and for 2 µm scale image is 27.3 nm.

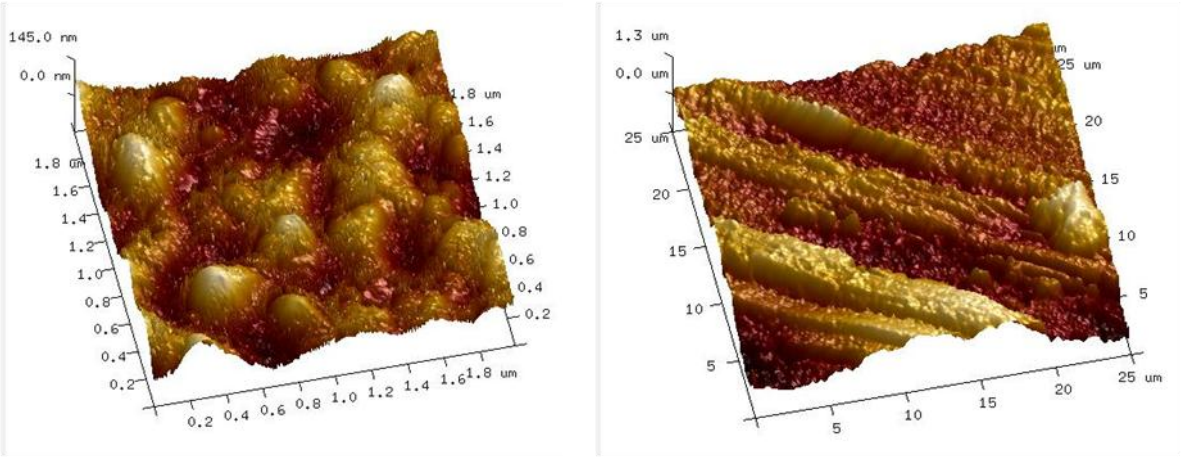

Figure 32: AFM image of “SS08” (HCl dipped) at different scales

Table 4: EDX data "SS08" (HCl dipped)

Elements	Composition by Weight %
C	0.7
N	3.66
Cr	16.43
Mn	3.13
Fe	69.45
Ni	6.64

Elemental composition we got from EDX of "SS08" (HCl dipped) substrate is almost same to the "SS00" substrate composition which is 16.24% Cr, 7.44% Ni. The difference is in the composition of magnesium which is 1.93% in "SS00" (untreated); this deviation can be due to less reactivity of Mn with HCl because of which surface atoms of Mn were not etch by HCl. Elemental compositions by weight have tabulated in Table 4 and EDX spectrum is shown in Fig.33.

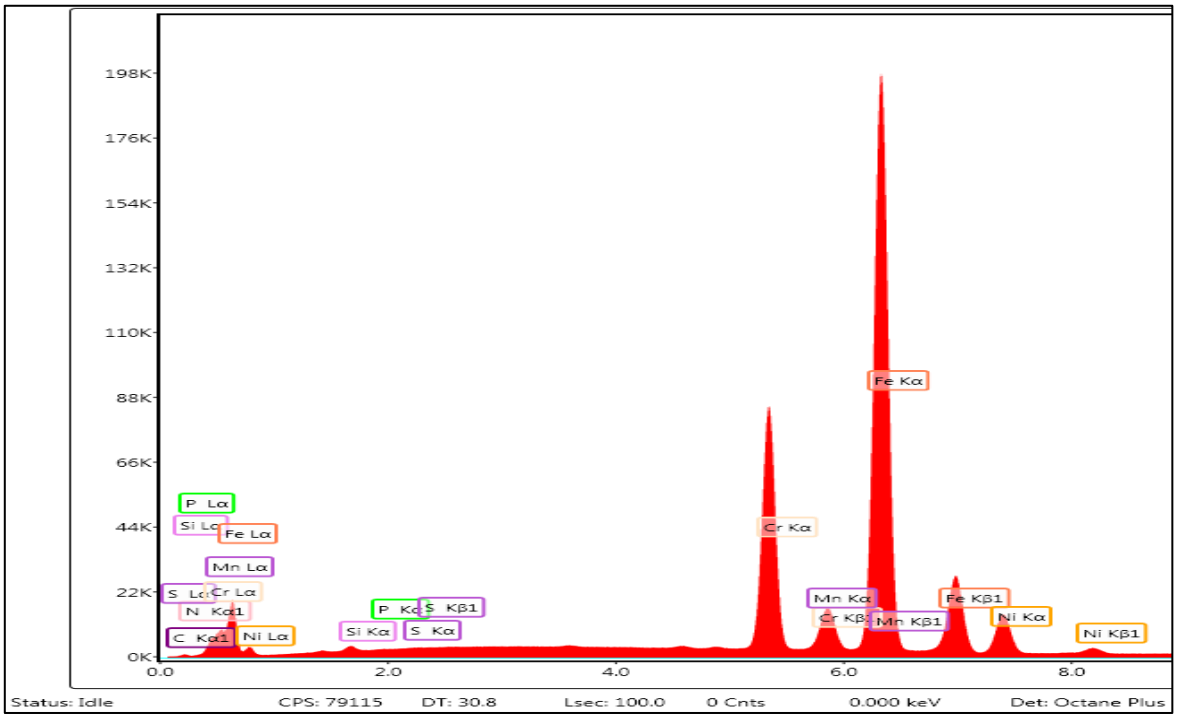

Figure 33: EDX spectrum "SS08" (HCl dipped)

“SS01”

“SS01” is the substrate from “Run 1” in pre CVD treatment substrate was sonicated in HCl for 10 min. CNTs were not found in this substrate which is confirmed by FESEM images in Fig. 34. Amorphous carbon gets deposited on the substrate due to diffusion of C_2H_2 on surface. Due to improper pre CVD treatment with HCl desired results was not achieved. Experiment was repeated with same parameters as “Run 2”.

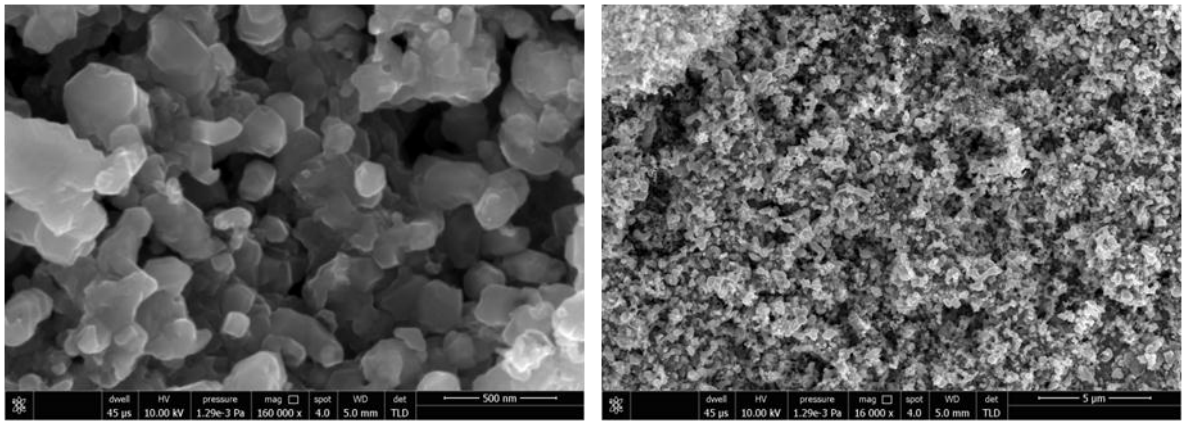

Figure 34: FESEM image of “SS01” at different magnifications

“SS02”

“SS02” is the substrate from “Run 1” in pre CVD treatment substrate was dipped in HCl for 10 min. CNTs were not found in this substrate which is confirmed by FESEM images in Fig. 35. Amorphous carbon gets deposited on the substrate due to diffusion of C_2H_2 on surface. Due to improper pre CVD treatment with HCl desired results was not achieved. Experiment was repeated with same parameters as “Run 2”.

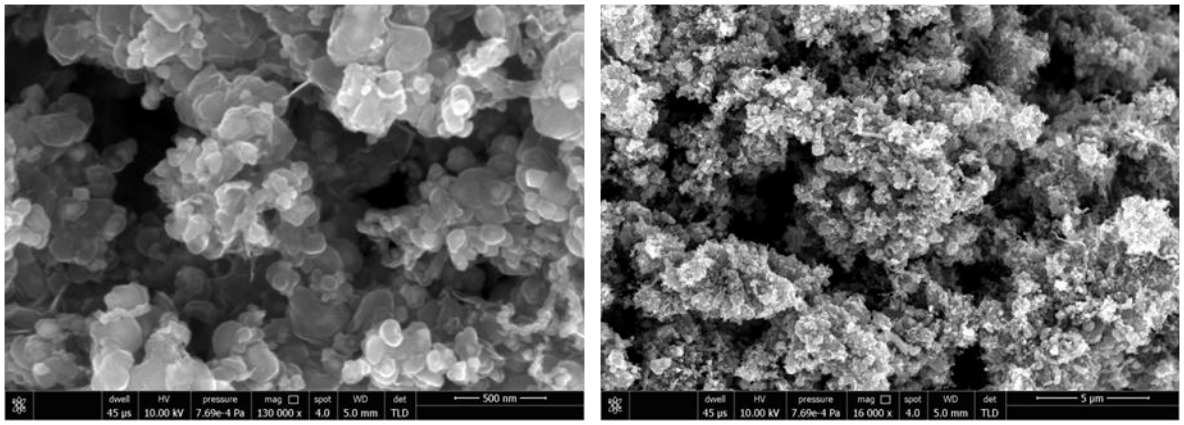

Figure 35: FESEM image of “SS02” (HCl dipped) at different magnifications

“SS03”

“SS03” is the substrate from “Run 1” in pre CVD treatment substrate was untreated. CNTs were found in this substrate but their density is too low and diameter of CNTs was large which is confirmed by FESEM images in Fig. 36. Desired results were not achieved. Experiment was repeated with same parameters as “Run 2”.

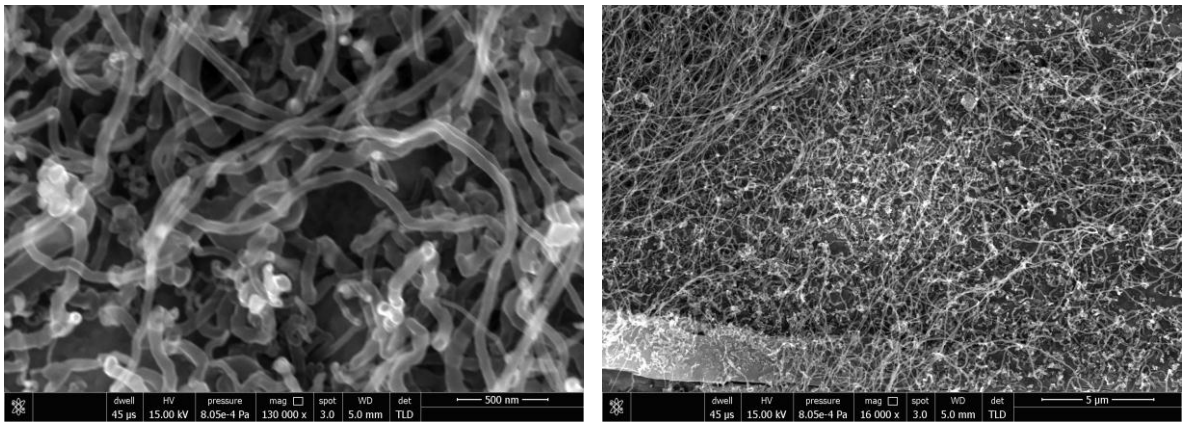

Figure 36: FESEM image of “SS03” (untreated) at different magnifications

"SS04"

"SS04" is the substrate from "Run 2" in pre CVD treatment substrate was sonicated in HCl for 10 min.

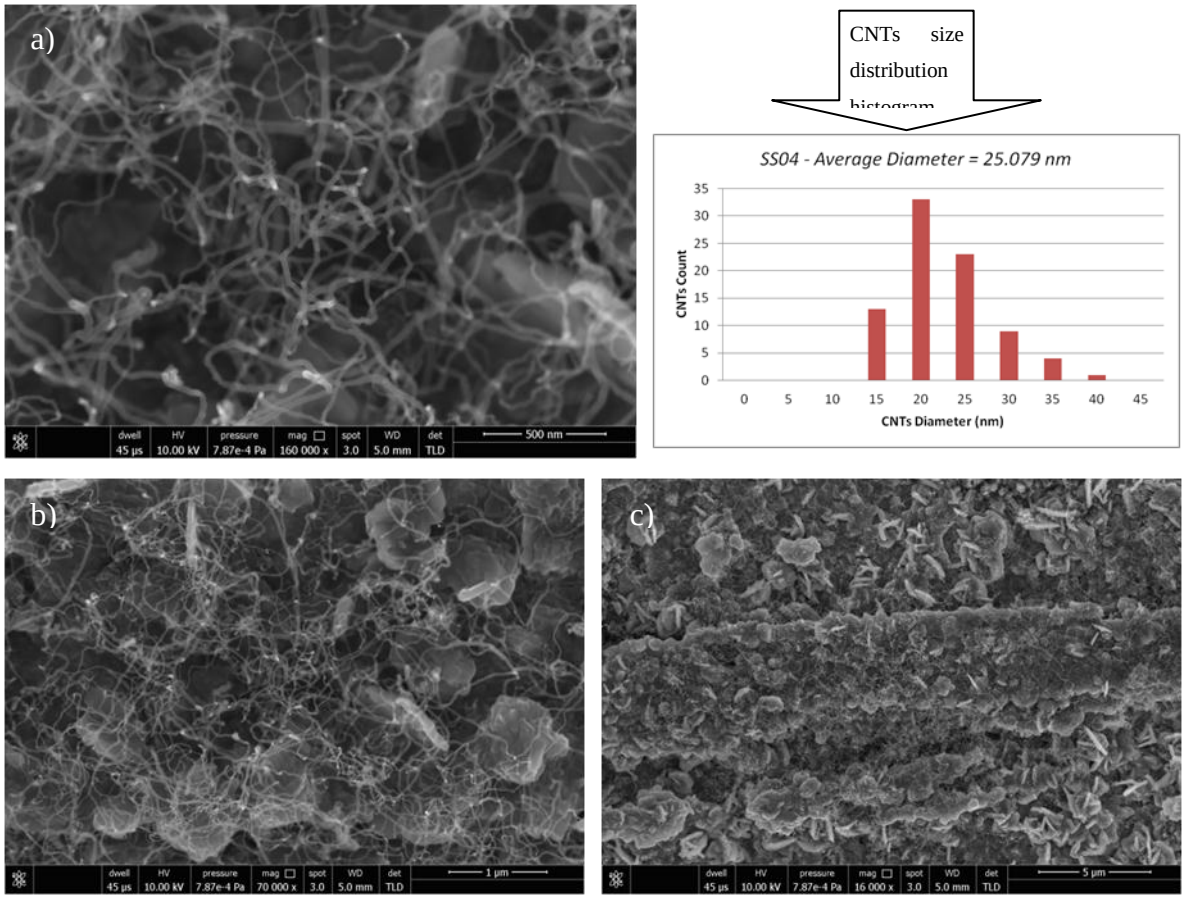

Figure 37: FESEM images of "SS04" (HCl sonicated) at different magnifications a), b), c) and CNTs size distribution histogram.

FESEM images in Fig. 37 shows growth of CNTs is there on "SS04" (HCl sonicated) substrate. Density of CNTs is too low and more amorphous carbon is there under CNTs mesh. Average CNT size calculated using imageJ software is 25.079 nm.

Table 5: EDX data of "SS04" (HCl sonicated)

Elements	Composition by Weight %
C	56.27
N	2.64
Cr	1.5
Mn	0.49
Fe	38.5
Ni	0.57

Elemental compositions by weight have tabulated in Table 4 and EDX spectrum is shown in Fig.38 which confirms the presence of large amount of carbon on the surface of "SS04" (HCl sonicated) substrate. Amount of chromium, iron and nickel is decreased significantly as a thick layer of carbon is deposited on the surface of stainless steel 304.

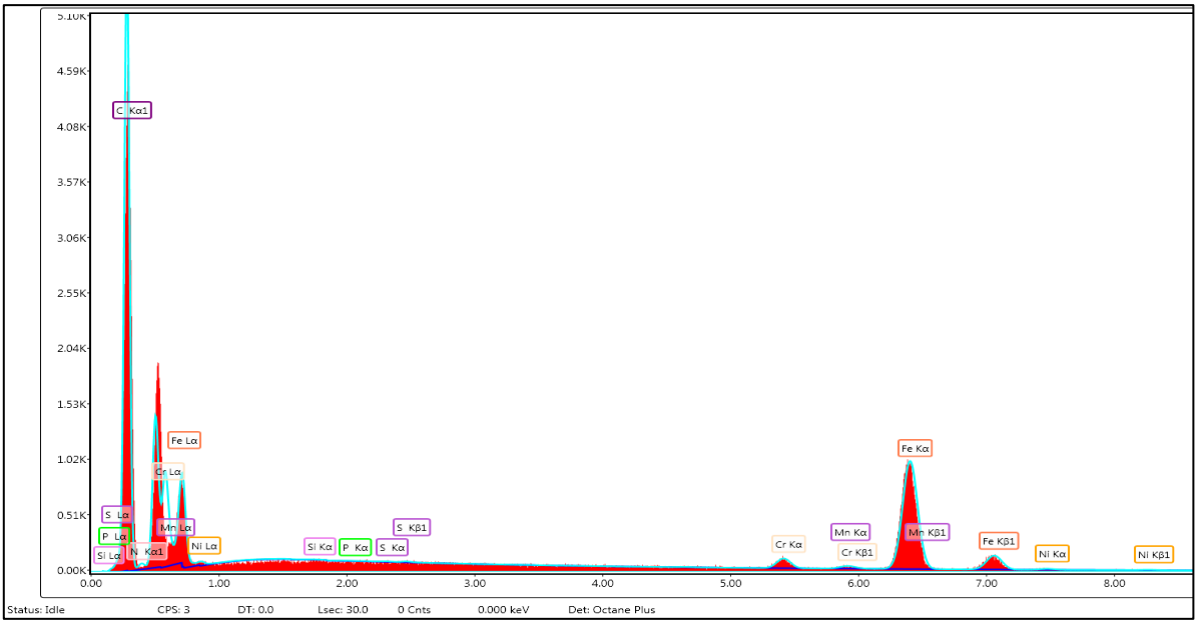

Figure 38: EDX spectrum of "SS04" (HCl sonicated)

"SS04s"

"SS04s" is the "SS04" (HCl sonicated) substrate whose surface is stripped by a blade so that layer of deposited material can be removed from the surface of stainless steel to investigate pre growth morphology of substrate.

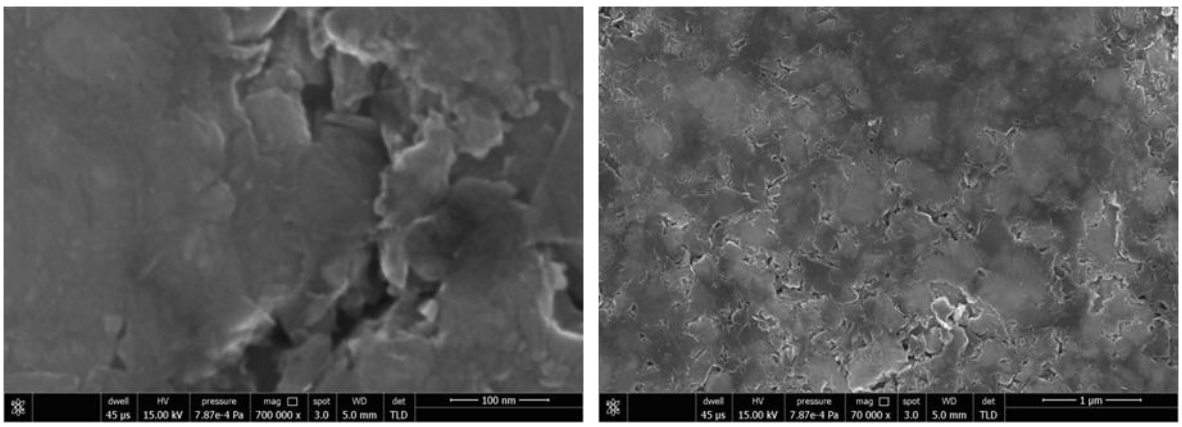

Figure 39: FESEM images of "SS04s" (HCl sonicated) at different magnifications

FESEM image in Fig. 39 shows flakes like structure which are forming a uniform layer on the surface of "SS04" (HCl sonicated). If we see near the cracked portions some small flakes are there. All thies may be contributing to the growth of CNTs.

Table 6: EDX data of "SS04s" (HCl sonicated)

Elements	Composition by Weight %
C	24.64
N	0.93
Cr	10.8
Mn	2.32
Fe	59.8
Ni	1.35

Elemental compositions by weight have tabulated in Table 6 and EDX spectrum is shown in Fig.40 which confirms the presence of significant amount of carbon on the surface of "SS04" (HCl sonicated) substrate. Amount of chromium, iron and nickel is increased as a thick layer of carbon is removed from the surface of stainless steel 304. This means a lot of carbon is defused to the bulk substrate.

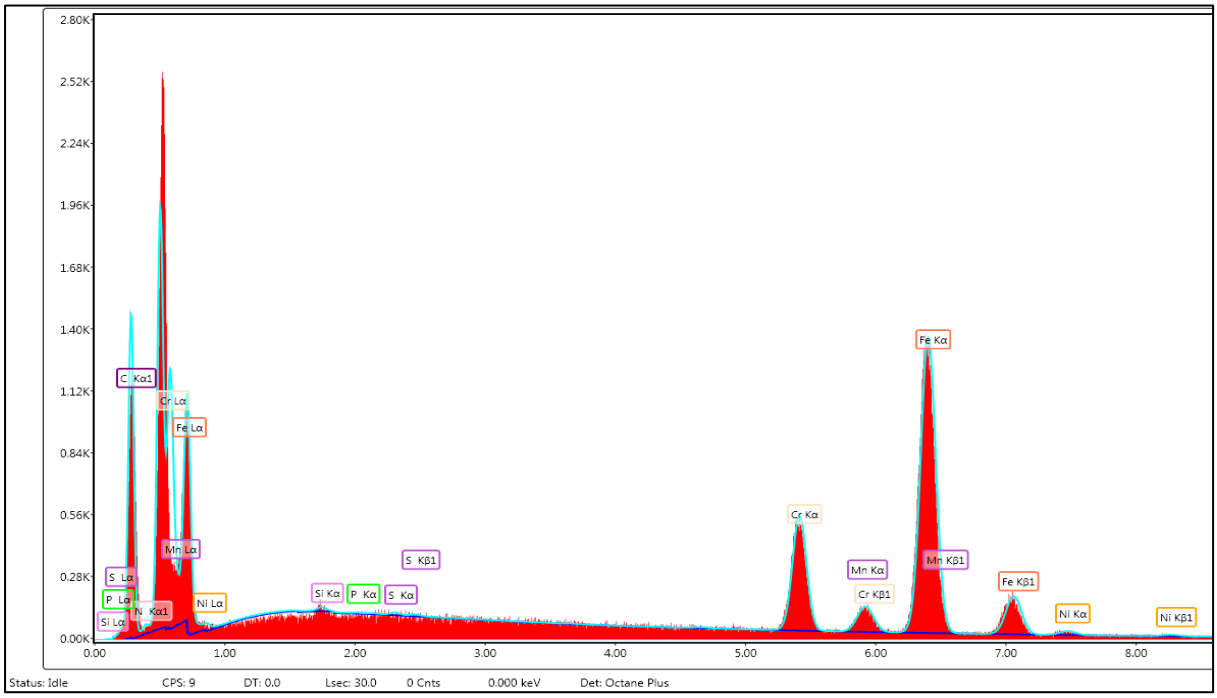

Figure 40: EDX spectrum of "SS04s" (HCl sonicated)

"SS05"

"SS05" is the substrate from "Run 2" in pre CVD treatment substrate was dipped in HCl for 10 min.

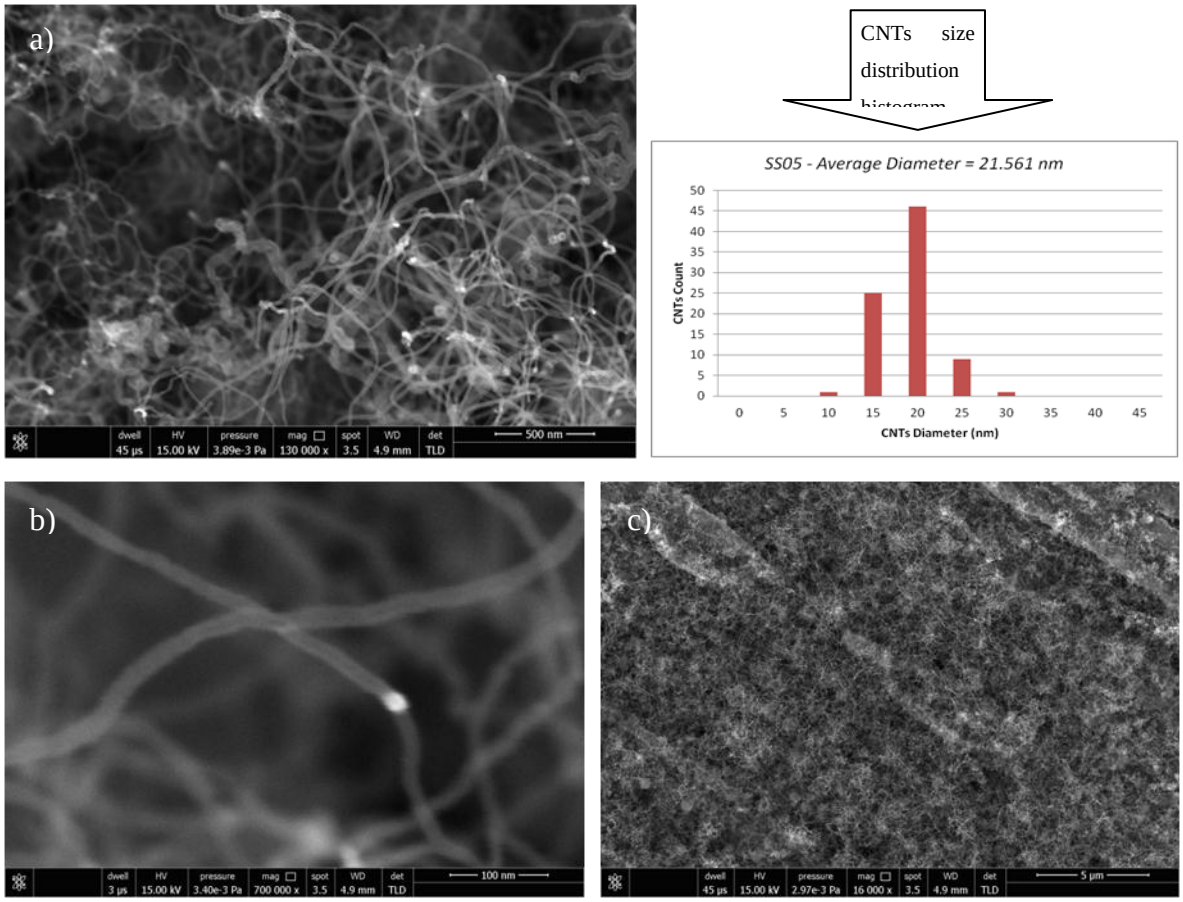

Figure 41: FESEM images of "SS05" (HCl dipped) at different magnifications a), b), c) and CNTs size distribution histogram.

FESEM images in Fig. 41 shows growth of CNTs is there on "SS05" (HCl dipped) substrate. Density of CNTs is low and amorphous carbon is not there under CNTs mesh. Average CNT size calculated using imageJ software is 21.561 nm.

Table 7: EDX data of "SS05" (HCl dipped)

Elements	Composition by Weight %
C	37.66
N	1.92
Cr	7.82
Mn	2.5
Fe	24.03
Ni	0.44

Elemental compositions by weight have tabulated in Table 7 and EDX spectrum is shown in Fig.42 which confirms the presence of large amount of carbon on the surface of "SS05" (HCl dipped) substrate. Amount of chromium, iron and nickel is decreased significantly as a thick layer of carbon material is deposited on the surface of stainless steel 304.

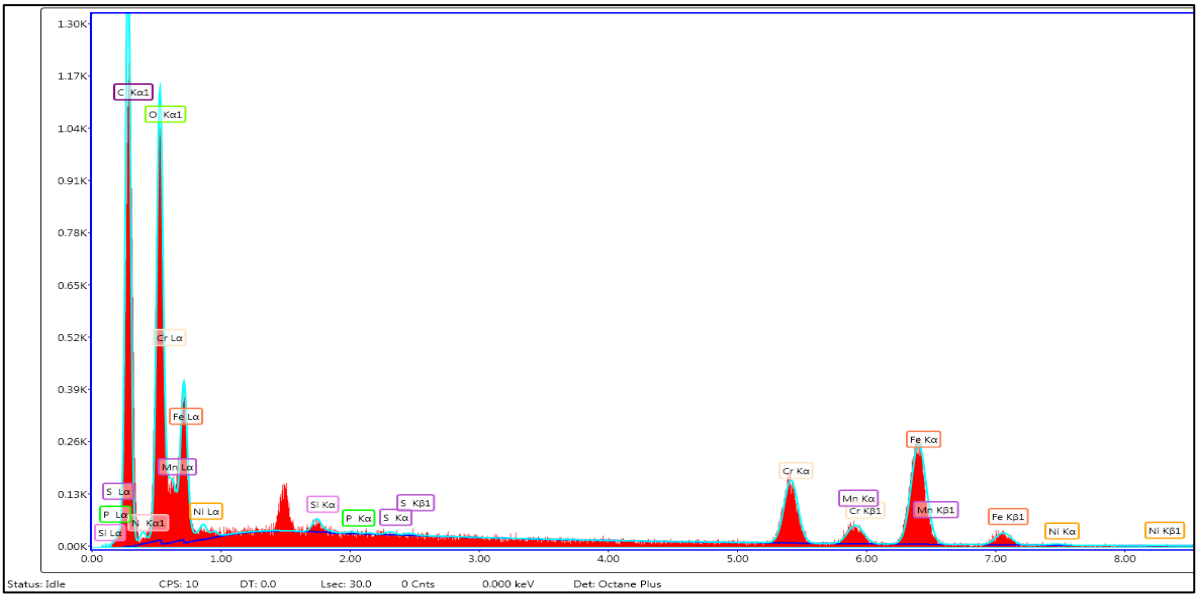

Figure 42: EDX spectrum of "SS05" (HCl dipped)

"SS05s"

"SS05s" is the "SS05" (HCl dipped) substrate whose surface is stripped by a blade so that layer of deposited material can be removed from the surface of stainless steel to investigate pre growth morphology of substrate.

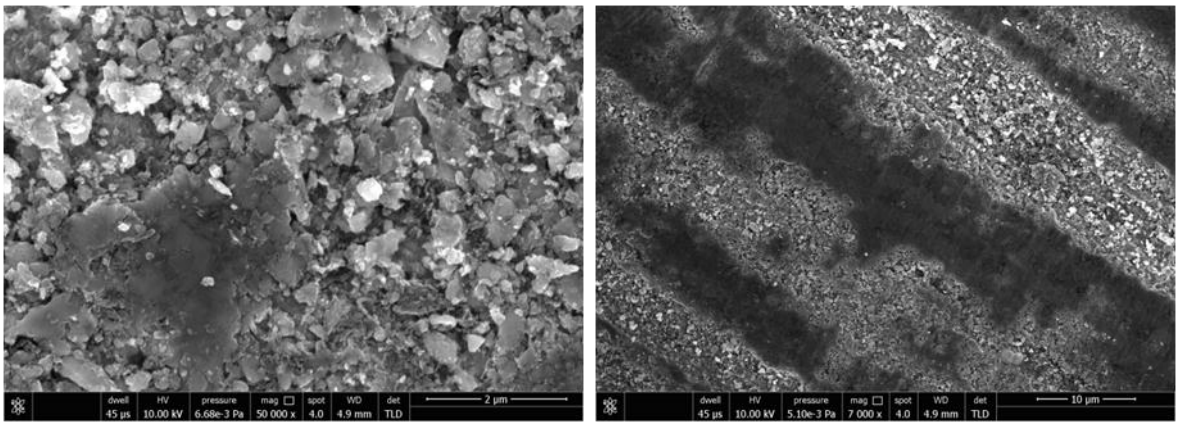

Figure 43: FESEM images of "SS05s" (HCl dipped) at different magnifications

FESEM image in Fig. 43 shows flakes like structure which were formed on the surface of "SS05" (HCl dipped) during anneling of substrate in argon atmosphere. If we see near the cracked portions some small flakes are there. All thies may be contributing to the growth of CNTs.

Table 8: EDX data of "SS05s" (HCl dipped)

Elements	Composition by Weight %
C	13
N	1.06
Cr	14.81
Mn	2.39
Fe	53.21
Ni	4.62

Elemental compositions by weight have tabulated in Table 8 and EDX spectrum is shown in Fig.44 which confirms the presence of significant amount of carbon on the surface of "SS05" (HCl dipped) substrate. Amount of chromium, iron and nickel is increased as a thick layer of carbon is removed from the surface of stainless steel 304. This means a lot of carbon is defused to the bulk substrate.

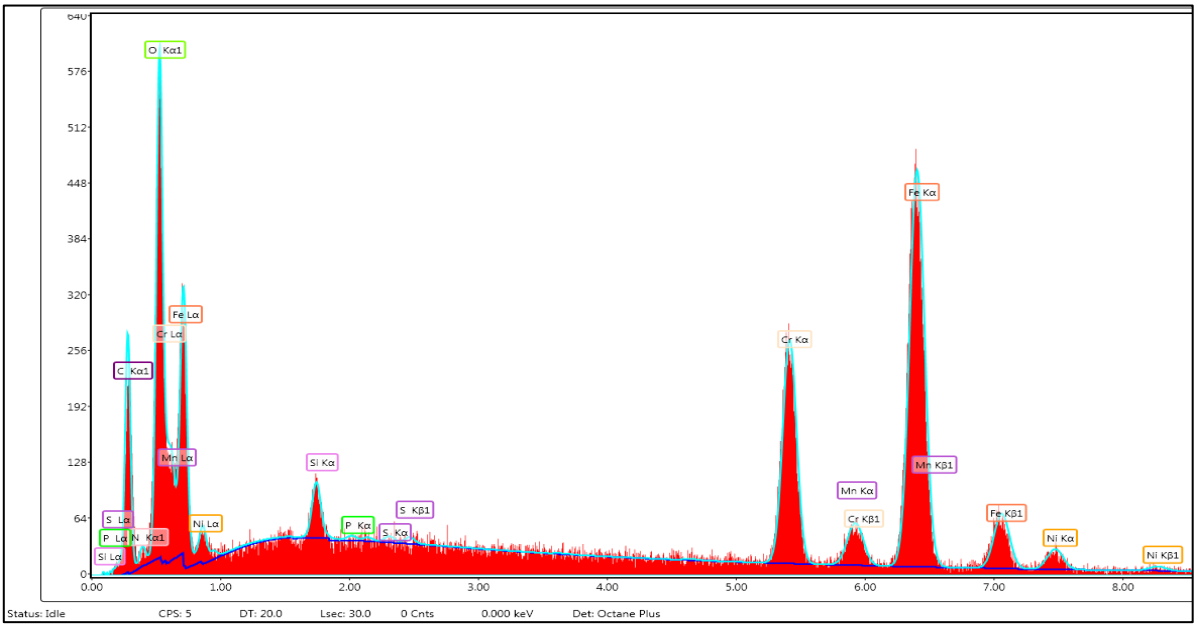

Figure 44: EDX spectrum of "SS05s" (HCl dipped)

"SS06"

"SS06" is the substrate from "Run 2" in pre CVD treatment substrate was untreated.

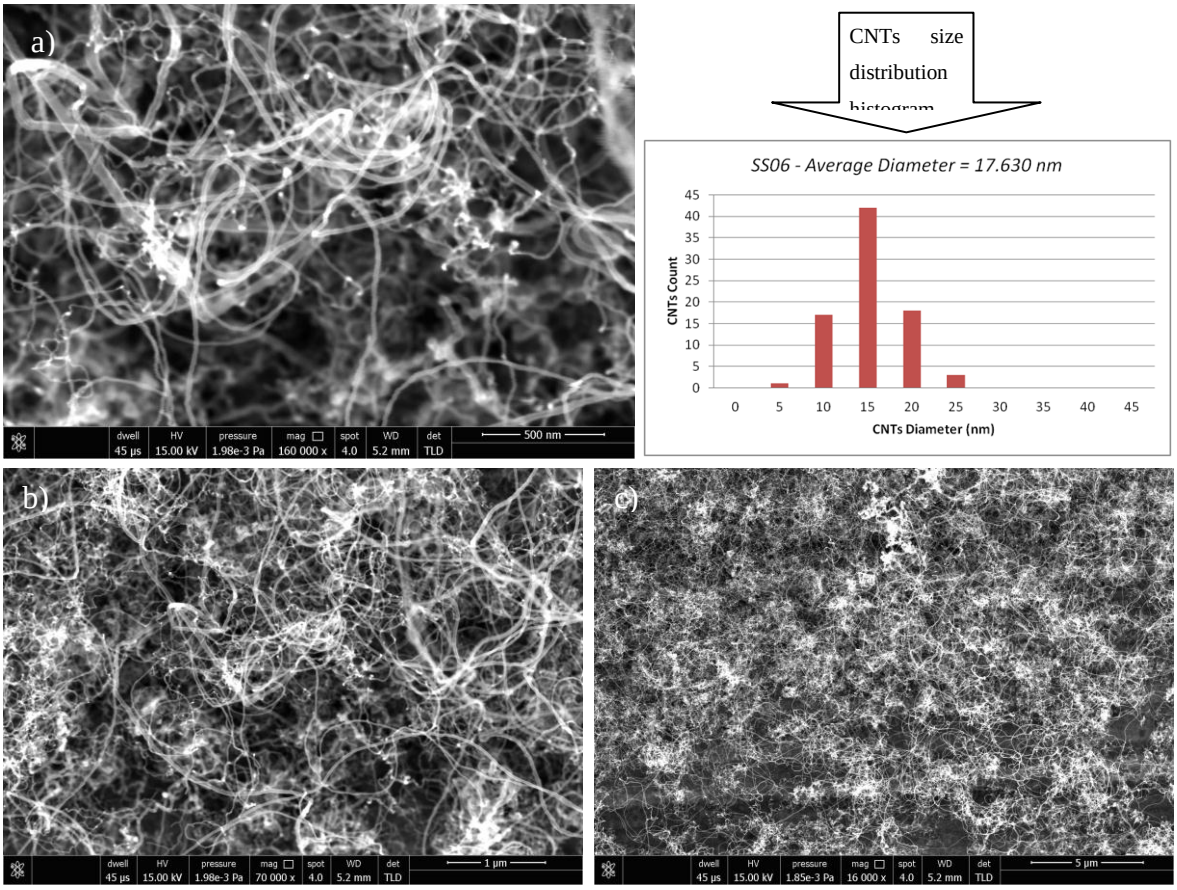

Figure 45: FESEM images of "SS06" (untreated) at different magnifications a), b), c) and CNTs size distribution histogram.

FESEM images in Fig. 45 shows growth of CNTs is there on "SS06" (untreated) substrate. Density of CNTs is high and amorphous carbon is not there under CNTs mesh. Average CNT size calculated using imageJ software is 17.630 nm.

Table 9: EDX data of "SS06" (untreated)

Elements	Composition by Weight %
C	17.18
N	1.72
Cr	14.99
Mn	2.48
Fe	47.49
Ni	4.6

Elemental compositions by weight have tabulated in Table 9 and EDX spectrum is shown in Fig.46 which confirms presence of small amount of carbon on the surface of "SS06" (untreated) substrate. Amount of chromium, iron and nickel is almost same as a thin layer of carbon material is deposited on the surface of stainless steel 304.

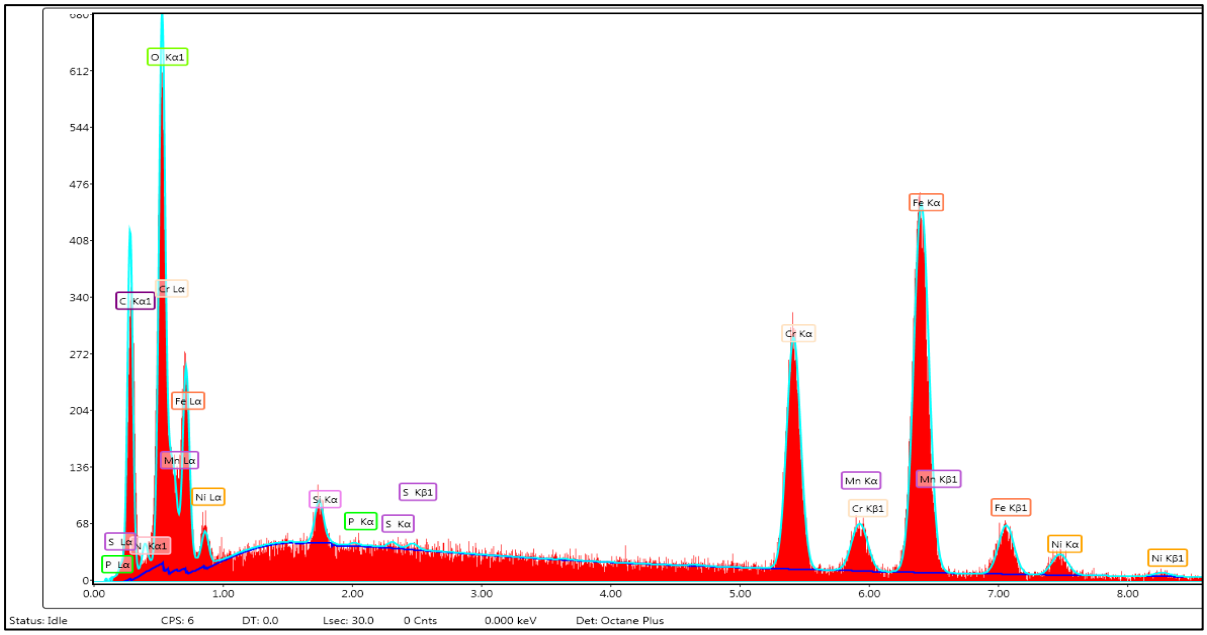

Figure 46: EDX spectrum of "SS06" (untreated)

"SS06s"

"SS06s" is the "SS06" (untreated) substrate whose surface is stripped by a blade so that layer of deposited material can be removed from the surface of stainless steel to investigate pre growth morphology of substrate.

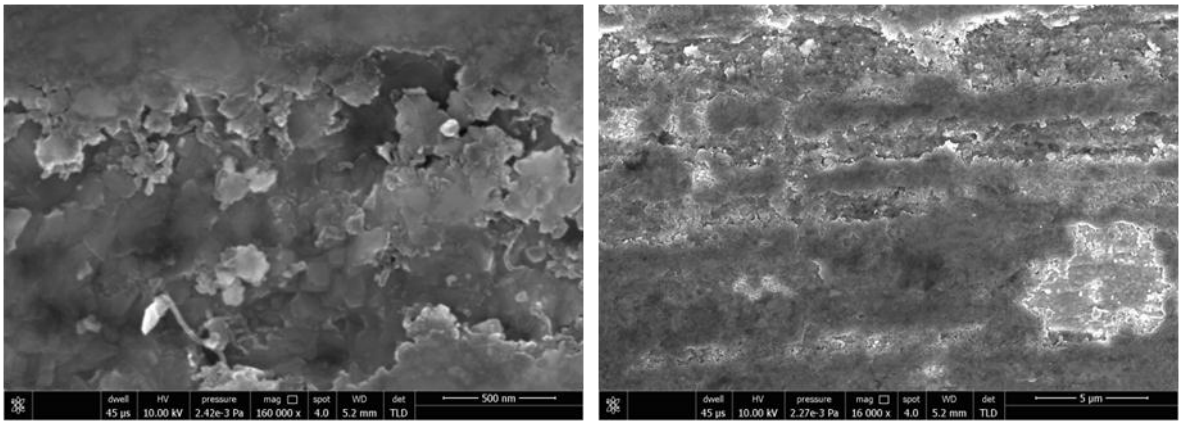

Figure 47: FESEM images of "SS06s" at different magnifications

FESEM image in Fig. 47 shows flakes like structure which were formed on the surface of "SS06" (untreated) during anneling of substrate in argon atmosphere. If we see near the cracked portions some small flakes are there. All thies may be contributing to the growth of CNTs.

Table 10: EDX data of "SS06s" (untreated)

Elements	Composition by Weight %
C	2.23
N	0.92
Cr	17.07
Mn	2.89
Fe	62.05
Ni	5.91

Elemental compositions by weight have tabulated in Table 9 and EDX spectrum is shown in Fig.48 which confirms presence of very low amount of carbon on the surface of "SS06" (untreated) substrate. Amount of chromium, iron and nickel is increased as a thin layer of carbon is removed from the surface of stainless steel 304. This means carbon is not much defused to the bulk substrate.

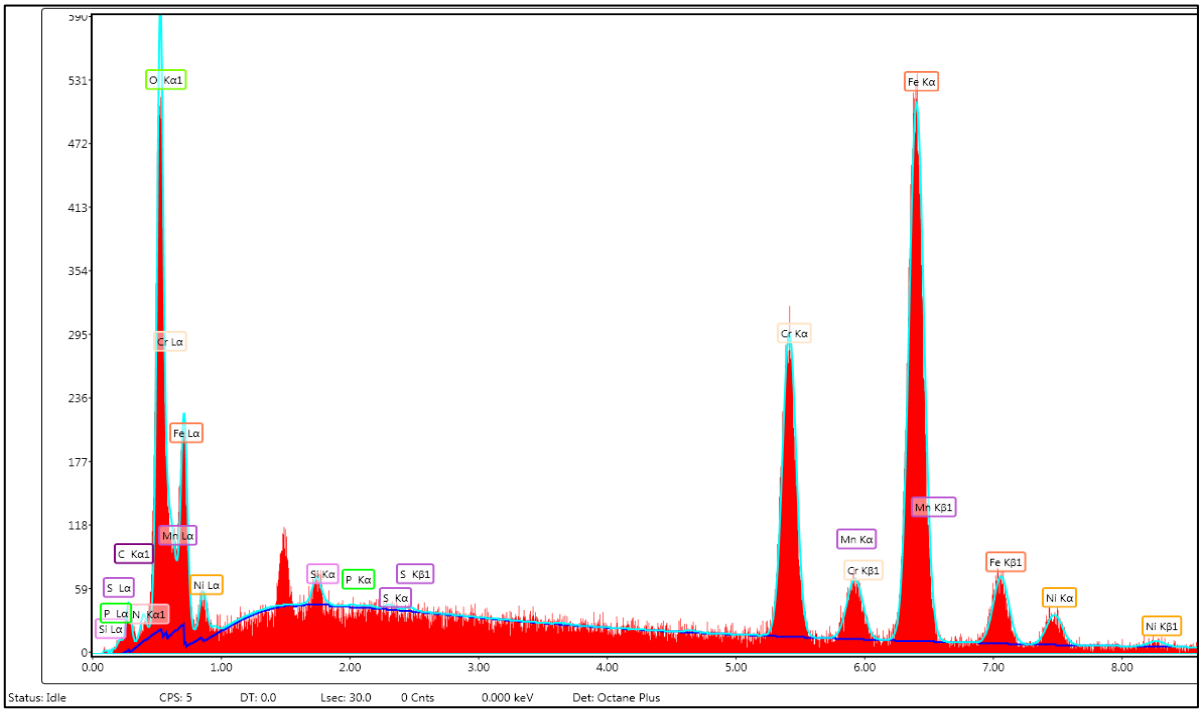

Figure 48: EDX spectrum of "SS06s" (untreated)

Discussion

Pre CVD Treatments

In this part we make a comparison between the changes in surface morphology of SS 304 substrates after getting treated by HCl.

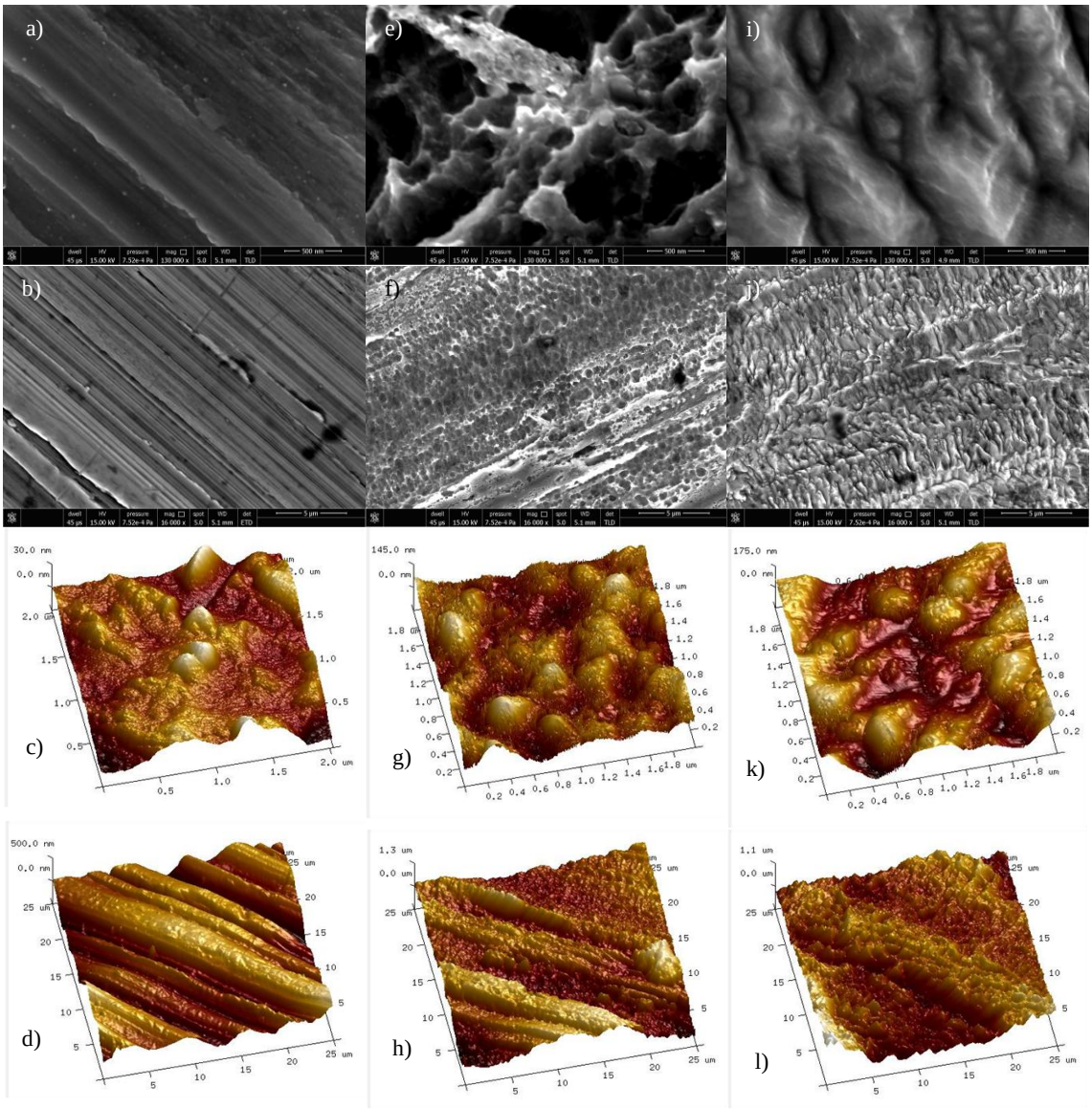

Figure 49: Comparison between surface morphology of SS 304 substrates after getting treated by HCl. Above are the FESEM and AFM images of [a-d]"SS00" (untreated), [e-h]"SS08" (HCl dipped), [i-l]"SS07" (HCl sonicated)

FESEM images we can see that polished SS 304 substrate get etch by HCl removing surface materials of substrate and making substrate surface porous in case of "SS08" (HCl dipped), in "SS07" (HCl sonicated) due to sonication in HCl a lot of surface material is etched that's why "SS08" surface lock like an unpolished steal surface. On comparing FESEM images we can interpret that surface nano features of "SS00" HCl untreated substrate is much smaller than "SS07" (HCl sonicated) and "SS08" substrate. And also "SS08" (HCl dipped) surface features look like a porous material whose surface features are quite smaller than "SS07"

(HCl sonicated) surface features. From AFM data we can see the depth of etching is more when we sonicate substrate in HCl ("SS07") that's why image Fig. 49 g) shows maximum height of 175 nm.

Table 11: Comparison of surface roughness (Ra) using AFM data

Substrate	Image Scale	Ra
"SS00" untreated	25µm	109nm
	2µm	5.19nm
"SS07" HCl sonicated	25µm	198nm
	2µm	37.7nm
"SS08" HCl dipped	25µm	252nm
	2µm	27.3nm

As depicted in Table 11 the roughness of HCl treated substrates and grinded substrate we can conclude that roughness is very high in HCl dipped substrates and low in HCl sonicated substrate, this deviation is because when we sonicate substrate, its surface get a lot mechanical vibrations due to which the etching depth and amount of material etched increases.

Table 12: Comparison of EDX data of "SS00" (untreated), "SS07" (HCl sonicated), "SS08" (HCl dipped) by weight%

Elements	"SS00"(w%)	"SS07"(w%)	"SS08"(w%)
C	3.24	3.51	0.7
N	1.89	0.75	3.66
Cr	16.24	16.76	16.43
Mn	1.93	2.13	3.13
Fe	68.92	69.64	69.45
Ni	7.44	7.01	6.64

Elemental composition we get from EDX of all this pre CVD treatment substrates are almost same; we can see that chromium is around 16-17%, iron is around 69%, nickel around 7% in all substrates. The most deviation is shown by composition of Mn in "SS08" (HCl dipped). this deviation can be due to less reactivity of Mn with HCl because of which surface atoms of Mn were not etch by HCl. Table 12 show elemental comparison of "SS00" (untreated), "SS07" (HCl sonicated), "SS08" (HCl dipped) by weight%.

Synthesis of Carbon Nanotubes

In this part we make a comparison between the growth of CNTs on differently pre CVD treated SS 304 substrates.

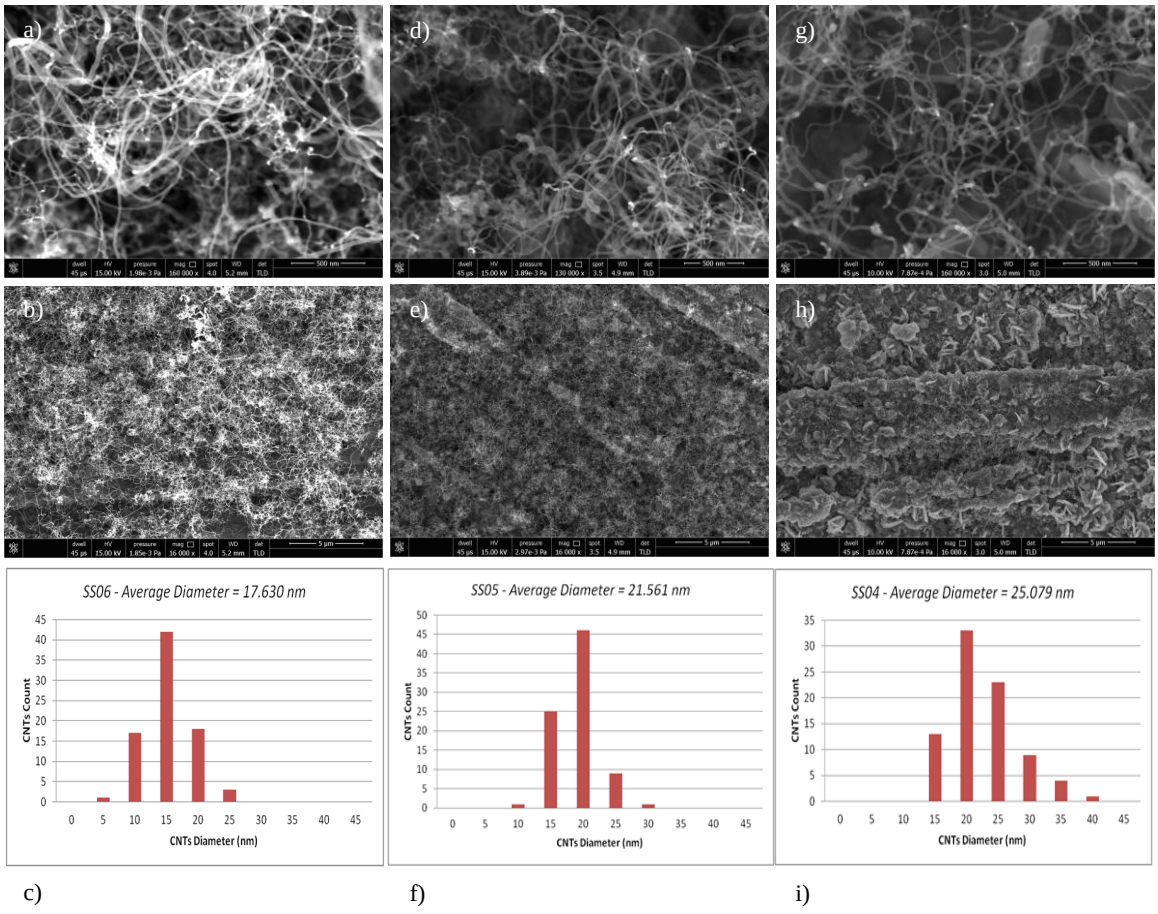

Figure 50: Comparison between the growth of CNTs on differently pre CVD treated SS 304 substrates. Above are the FESEM images of [a,b]"SS04" (HCl sonicated), [d,e]"SS05" (HCl dipped), [g,h]"SS06" (untreated)

A FESEM image in Fig. 50 confirms presence of CNTs on each substrates we put in CVD for CNTs growth. What deviations we see due to pre CVD treatments are in terms of CNTs average diameter, CNTs density and amorphous carbon coverage. "SS04" which is HCl sonicated substrate shows 25.079 nm CNTs average diameter, less CNTs density and more amorphous carbon coverage; it can be due to bulk diffusion of C_2H_2 in SS 304 substrate. "SS05" which is HCl dipped substrate shows 21.561 nm CNTs average diameter, less CNTs density and less amorphous carbon coverage; it can be due to porous SS 304 surface formed in pre CVD treatments, as the surface area is more it won't allow bulk diffusion of C_2H_2 in SS 304 substrate, diffusion is more on surface. "SS06" which is HCl untreated substrate shows 17.630 nm CNTs average diameter, more CNTs density and very less amorphous

carbon coverage; it can be due to grinded surface of the SS 304 substrate, as the surface is very fine, it would not allow bulk diffusion of C_2H_2 in SS 304 substrate. After striping these substrates with blade all substrate surfaces shows somewhere flat and uniform layers and somewhere flakes like structures.

Table 13: Comparison of EDX data of "SS04" (HCl sonicated), "SS04s", "SS05" (HCl dipped), "SS05s", "SS06" (untreated), "SS06s" by weight%

Elements	"SS04s"(w%)	"SS05s"(w%)	"SS06s"(w%)	"SS04"(w%)	"SS05"(w%)	"SS06"(w%)
C	24.64	13	2.23	56.27	37.66	17.18
N	0.93	1.06	0.92	2.64	1.92	1.72
Cr	10.8	14.81	17.07	1.5	7.82	14.99
Mn	2.32	2.39	2.89	0.49	2.5	2.48
Fe	59.8	53.21	62.05	38.5	24.03	47.49
Ni	1.35	4.62	5.91	0.57	0.44	4.6

Table 13 show EDX data of "SS04" (HCl sonicated), "SS04s", "SS05" (HCl dipped), "SS05s", "SS06" (untreated) and "SS06s" by weight % the element on which we should focus this time is carbon, lot of variations are there in concentration of carbon. After striping "SS04" (HCl sonicated), "SS05" (HCl dipped), "SS06" (untreated) substrates all carbon material is removed and what all left is the diffused carbon in substrate surface with this we can interpret that diffusion of carbon on the substrate is more in "SS04s" substrate, less in "SS05s" substrate and least in "SS06s" substrate. And that's why we saw more amorphous carbon on "SS04" (HCl sonicated) substrate.

Chapter-5 CONCLUSION AND FUTURE SCOPE

Conclusion and Future Scope

Different pre CVD treatment procedures were applied on the substrate surface and their effects on CNTs growth were investigated. It was found that best results for CNTs growth is shown on untreated substrate ("SS06") with average CNTs diameter 17.630 nm and also quite dense CNTs growth is there on "SS06" substrate. "SS04" which is HCl sonicated shows maximum amount of amorphous carbon deposited on SS 304 substrate.

More pre-treatments can be performed on SS 304 substrates to get vertically aliened dense forest of CNTs which can be used as an electrode material for applications like fuel cells, supper capacitors, batteries, solar cells, etc. CNTs grown on stainless steel can be functionalize and doped with other elements can enhance the above applications.

REFERENCES

1. The era of carbon allotropes, Andreas Hirsch, Nature Materials,9868-871(2010).
2. Recent Progress on the Growth Mechanism of Carbon Nanotubes: A Review, Jean-Philippe Tessonnie and Dang Sheng Su, Chem Sus Chem 0000, 00, 1 – 25(2011).
3. Lee, Cheol Jin, Lyu, Seung Chul, Kim, Hyoun Woo, Park, Chong Yun, and Yang, Cheol Woong,, Chemical Physics Letters, 359, (1,2), 2002
4. Springer handbook of nanotechnology, Professor Bharat Bhushan Nano tribology Laboratory.
5. Breuer, O. and U. Sundararaj, Big returns from small fibres: a review of polymer/carbon nanotube composites. Polymer composites, 2004. 25(6): p. 630-645.
6. Yadav, B.C. and R. Kumar, Structure, properties and applications of fullerenes. International Journal of Nanotechnology and Applications, 2008. 2(1): p. 15-24.
7. Krueger, A., Carbon materials and nanotechnology: Wiley-VCH.
8. Buchachenko, A.L., Nanochemistry: a direct route to high technologies of the new century. Russian chemical reviews, 2003. 72(5): p. 375-391.
9. Coluci, V.R., D.S. Galvao, and A. Jorio, Geometric and electronic structure of carbon nanotube networks: 'super'-carbon nanotubes. Nanotechnology, 2006. 17(3): p. 617.
10. Belin, T. and F. Epron, Characterization methods of carbon nanotubes: a review. Materials Science and Engineering: B, 2005. 119(2): p. 105-118.
11. Sugai, T., et al., New synthesis of high-quality double-walled carbon nanotubes by high-temperature pulsed arc discharge. Nano Letters, 2003. 3(6): p. 769-773.
12. T. Guo, P. Nikolaev, A. Thess, D.T. Colbert, R.E. Smalley Chemical Physics Letters 243 (1995) 49-54
13. A. Thess, R. Lee, P. Nikolaev, H. Dai, P. Petit, J. Robert, C. Xu, Y. H. Lee, S. G. Kim, A. G. Rinzler, D. T. Colbert, G. E. Scuseria, D. Tomanek, J. E. Fischer and R. E. Smalley: Science 273 (1996) 483.
14. Yudasaka, M., Yamada, R., Sensui, N., Wilkins, T., Ichihashi, T., and Iijima, S., Journal of Physical Chemistry B, 103, (30), 1 999
15. Eklund, P. C., Pradhan, B. K., Kim, U. J., Xiong, Q., Fischer, J. E., Friedman, A. D., Holloway, B. C., Jordan, K., and Smith, M. W., Nano Letters, 2, (6),2002.
16. Thess, A., Lee, R., Nikolaev, P., Dai, H.J., Petit, P., Robert, J., Xu, C.H., Lee, Y.H., Kim, S.G., Rinzler, A.G., Colbert, D.T., Scuseria, G.E., Tomanek, D., Fischer, J.E., and Smalley, R.E., Crystalline ropes of metallic carbon nanotubes, Science 273, 483–487, 1996.
17. Tang, Z.K., et al., Superconductivity in 4 Angstrom Single-Walled Carbon Nanotubes. Science, 2001. 292(5526): p. 2462-2465.
18. Kumar M Fau - Ando, Y. and Y. Ando, Chemical vapor deposition of carbon nanotubes: a review on growth mechanism and mass production. (1533-4880 (Print).
19. Carbon Nanotubes: Properties and Applications, By Michael J. O'Connell.
20. Carbon nanotube growth mechanism switches from tip- to base-growth with decreasing catalyst particle size, A. Gohiera, C.P. Ewelsa, T.M. Mineab, M.A. Djouadia, CARBON 4 6 (2008)1331–1338.
21. M Meyyappan, Lance Delzeit, Alan Cassell and David Hash, Carbon nanotube growth by PECVD: a review, 2003 Plasma Sources Sci. Technol. 12 205
22. Structure, Bonding, and Mineralogy of Carbon at Extreme Conditions, Artem R. Oganov, Russell J. Hemley and Robert M. Hazen, Adrian P. Jones.
23. UnderstandingNano.com, what is CNTs.
24. http://www.danablankenhorn.com/2008/05/how-dangerous-a.html.
25. Polymer/Carbon Nanotube Nano composites, Veena Choudhary and Anju Gupta.
26. http://commons.wikimedia.org/wiki/File:Arc_discharge_nanotube.png.
27. www.school-labs.com/t3694.html.

28. http://ipn2.epfl.ch/CHBU/NTproduction1.htm.
29. Carbon Nanotube Synthesis and Growth Mechanism, Mukul Kumar, Department of Materials Science &Engineering Meijo University, Nagoya 468-8502, Japan.
30. Carole E. Baddour, Faysal Fadlallah, Deniz Nasuhoglu, Reema Mitra, Leron Vandsburger, Jean-Luc Meunier, Carbon, Volume 47, Issue 1, January 2009, Pages 313-318
31. Yaping Zhang, Jian Sun, Yongyou Hu, Sizhe Li, Qian Xu, Journal of Power Sources, Volume 239, 1 October 2013, Pages 169-174
32. Dilip K. Singh, P.K. Iyer, P.K. Giri, Diamond and Related Materials, Volume 19, Issue 10, October 2010, Pages 1281-1288
33. Mazdak Hashempour, Antonello Vicenzo, Fu Zhao, Massimiliano Bestetti, Carbon, Volume 63, November 2013, Pages 330-347
34. Noriaki Sano, Takeshi Kodama, Hajime Tamon, Carbon, Volume 55, April 2013, Pages 365-368
35. Mazdak Hashempour, Antonello Vicenzo, Fu Zhao, Massimiliano Bestetti, Materials Characterization, Volume 92, June 2014, Pages 64-76
36. Nathan Hordy, Norma-Yadira Mendoza-Gonzalez, Sylvain Coulombe, Jean-Luc Meunier, Carbon, Volume 63, November 2013, Pages 348-357
37. N. Sabeti Nejad, M.M. Larijani, M. Ghoranneviss, P. Balashabadi, A. Shokouhy, Surface and Coatings Technology, Volume 203, Issues 17–18, 15 June 2009, Pages 2510-2513
38. Eui-Chul Shin, Goo-Hwan Jeong, Thin Solid Films, Volume 521, 30 October 2012, Pages 102-106
39. Noriaki Sano, Suguru Yamamoto, Hajime Tamon, Carbon, Volume 50, Issue 15, December 2012, Pages 5628-5630